

Supporting Information

Fully recyclable Pluripotent Networks for 3D printing enabled by dissociative dynamic bonds

Marco Caliari,^{a,b} Fernando Vidal,^a Daniele Mantione,^{a,c} Guillem Seychal,^{a,d} Mariano Campoy-Quiles^e, Lourdes Irusta,^a Mercedes Fernandez,^a Xabier Lopez de Pariza,^a Thomas Habets,^b Nora Aramburu,^a Jean-Marie Raquez,^d Bruno Grignard,^{b,f} Alejandro J. Müller,^{a,c} Christophe Detrembleur,^{b,g*} and Haritz Sardon^{a*}.

^aPOLYMAT and Department of Polymers and Advanced Materials: Physics, Chemistry and

Technology, Faculty of Chemistry, University of the Basque Country UPV/EHU, Paseo Manuel de

Lardizábal, 3, 20018 Donostia-San Sebastián, Spain. ^b Center for Education and Research on

Macromolecules (CERM), CESAM Research Unit, University of Liege, Sart-Tilman B6a, 4000

Liege, Belgium. ^cIkerbasque, Basque Foundation for Science, Plaza Euskadi 5, 48009, Bilbao.^d

Laboratory of Polymeric and Composite Materials, Center of Innovation and Research in Materials

and Polymers (CIRMAP), University of Mons, Place du Parc 23, Mons, 7000, Belgium. ^eInstitute of

Materials Science of Barcelona, ICMAB-CSIC, Campus UAB, 08193, Bellaterra, Spain. ^fFRITCO2T

Platform, University of Liege, Sart-Tilman B6a, 4000 Liege, Belgium. ^gWEL Research Institute,

Avenue Pasteur 6, 1300 Wavre, Belgium.

S1. Materials and Methods

S1.1 Materials

2-Methyl-3-butyn-2-ol (Sigma, 98%), Allylamine (Sigma, 98%), Copper Iodide (Sigma, 98%), Methyl 3-mercaptopropionate (Sigma, 98%, S1), Phenylbis(2,4,6-trimethylbenzoyl) phosphine oxide (BAPO, Ciba), Methanesulfonic acid (Sigma, >99%), Bis(4-methylphenyl)iodonium Hexafluorophosphate (IOD, Sigma, >99%, electronic grade), Isopropyl Thioxanthone (ITX, TCI, >98%), 1,3,5-trimethoxy benzene (Sigma) Trimethylolpropane tris(3-mercaptopropionate) (S3, Sigma, ≥95%), Pentaerythritol tetrakis(3-mercaptopropionate) (S4, Sigma, ≥95%), Dipentaerythritol Hexakis(3-mercaptopropionate) (S6, TCI, >93%), Triflic Acid (Sigma, >99%) and Sulfuric Acid (Sigma, >95%), Triethylamine (Sigma, 99.5%) were used without further purification.

S1.1.1 Synthesis AlLOx

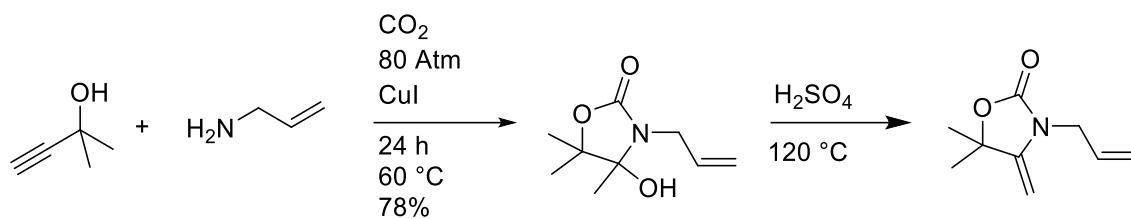


Figure S1. Synthesis of AlloX

3-allyl-5,5-dimethyl-4-methylenetetrahydro-2H-pyran-2-one (AlloX) was prepared by adapting Jiang *et al.* procedure.¹ 2-Methyl-3-butyn-2-ol (84.1 g, 100 mmol, 1 eq), allyl Amine (60 g, 105 mmol, 1.05 eq) and copper iodide (10 g, 5 mol%) were loaded in a stainless-steel autoclave. CO_2 was injected at a pressure of 80 atm and a temperature of 60 °C under mechanical stirring. After 24 h the reaction vessel was depressurized, and the deep red mixture was distilled with a short path distillation apparatus at 120 °C over sulfuric acid (0.5 mL) under vacuum. The target material was obtained as a colorless oil (130 g, 78% yield) and stored in a freezer (-18 °C).

$^1\text{H-NMR}$ (300 MHz, $\text{DMSO}-d_6$) δ 5.76 (m, 1H), 5.26 – 4.99 (m, 2H), 4.22 – 4.10 (m, 3H), 4.02 (dt, $J = 5.0, 1.7$ Hz, 2H), 1.47 (s, 9H). **$^{13}\text{C-NMR}$** (75 MHz, DMSO) δ 154.48, 149.72, 131.17, 116.58, 81.92, 80.31, 42.82, 27.52. **IR:** 2980, 1760, 1680, 1642. **Mp (DSC):** 6 °C.

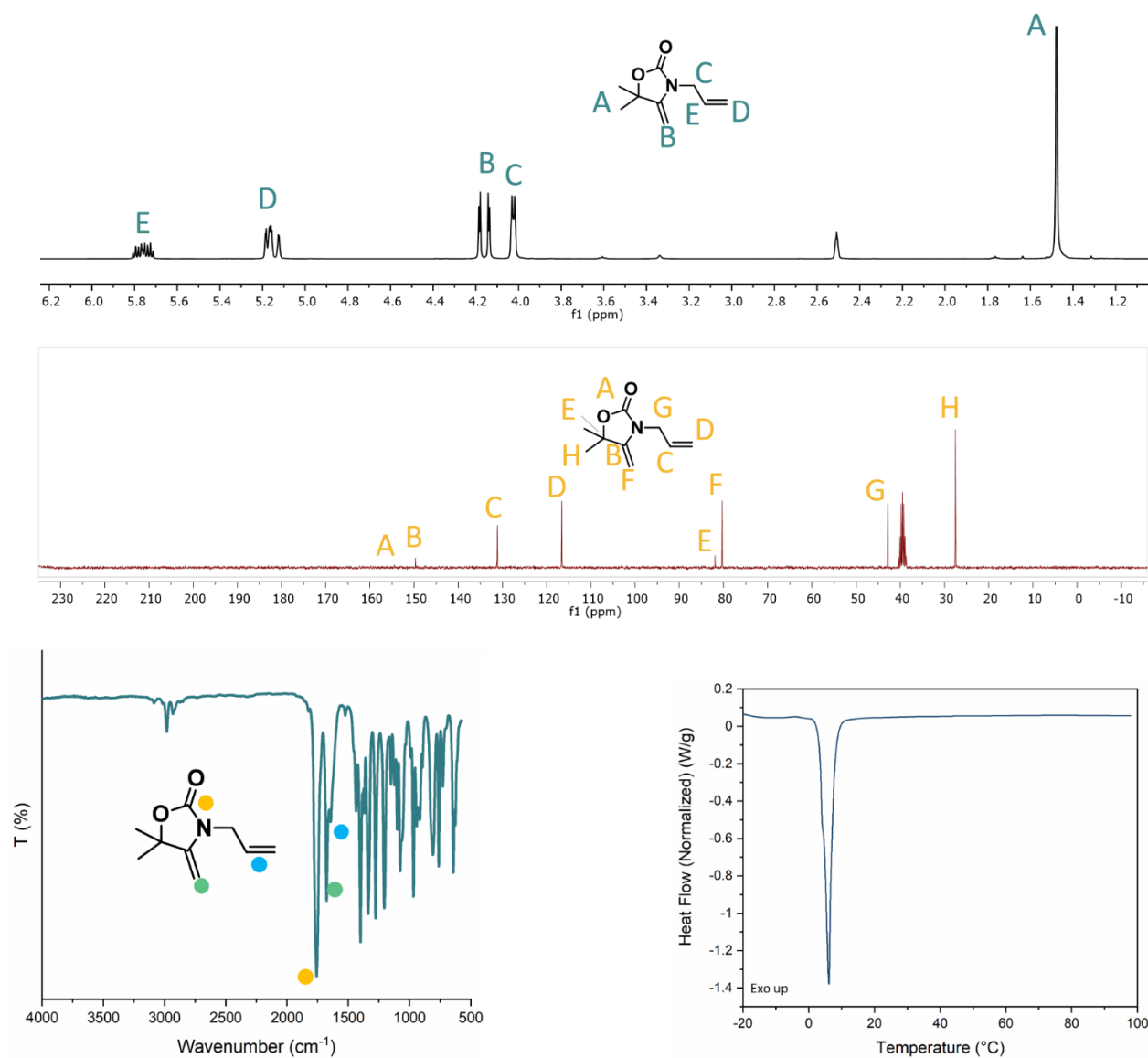


Figure S2. Characterisation of AlloX: ^1H -NMR, ^{13}C NMR, IR, DSC.

S1.1.3 Thiol ene reaction mechanism

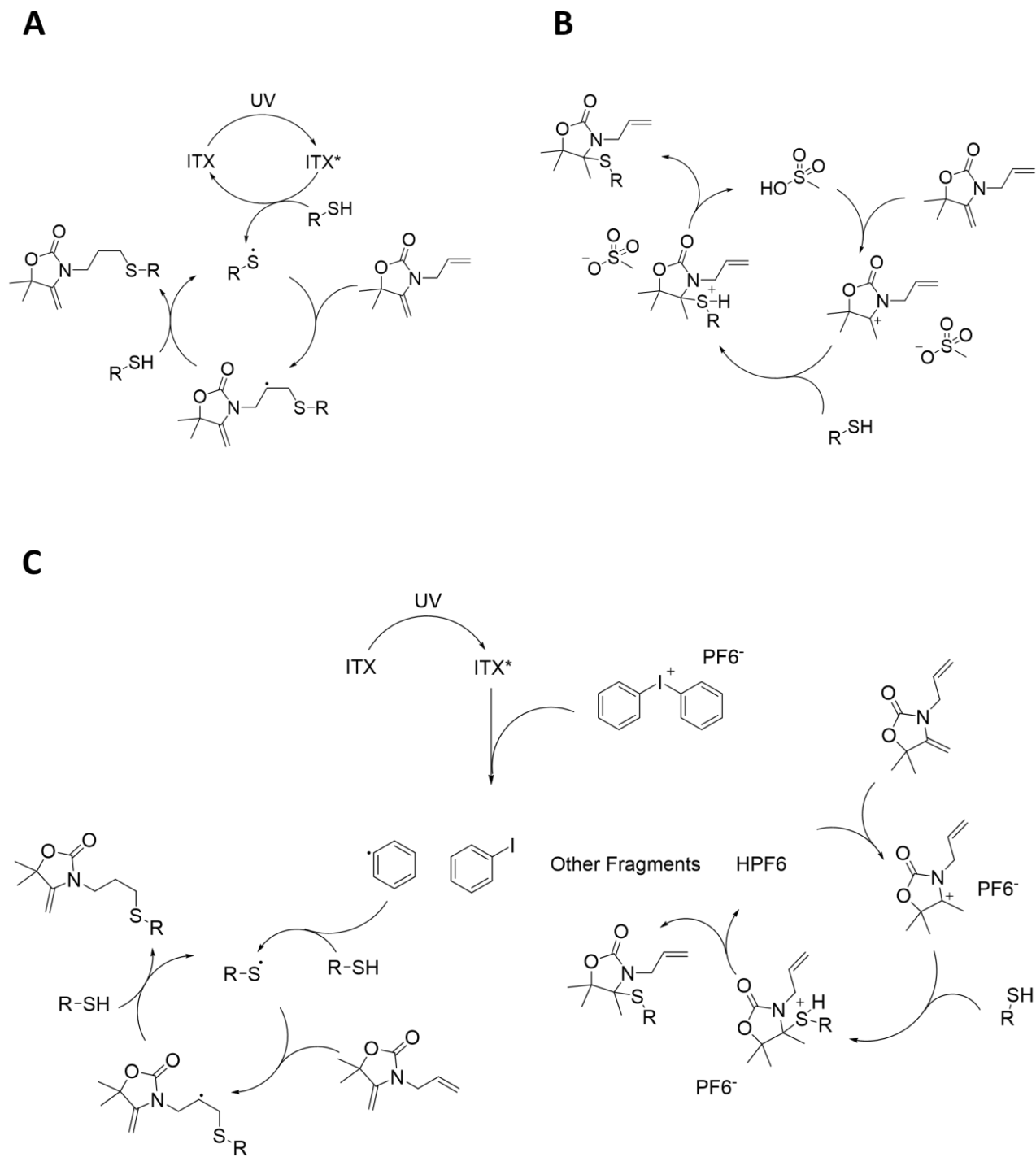


Figure S3. Reaction mechanism of radical thiol ene (a), cationic thiol ene (b) and tandem thiol ene (c) on AlloX. In (a) and (c) the reaction with the exocyclic double bond was omitted for brevity

S1.1.4 Synthesis radical model compounds OX_S1

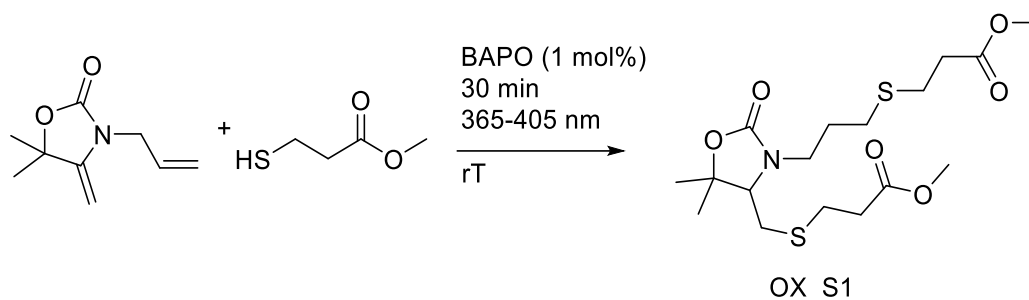


Figure S4. Synthesis of OX_S1

Allox (0.6 mmol, 1 eq) was mixed with methyl-3-mercaptopropionate (1.2 mmol, 2 eq) in a glass vial. BAPO (1 mol%) was dissolved in a small amount of dichloromethane and then added to the mixture. The homogenous yellow mixture was irradiated in an asiga flash curing chamber 30 min under stirring (Low pressure mercury lamp, 365-405 nm, 36 Watts). The resulting transparent mixture was diluted in EtOAc and was washed twice with subsaturated brine. The organic phases were dried over MgSO₄ and evaporated using rotary evaporation. The resulting yellow viscous liquid was subjected to column chromatography (Hex:EtOAc 7:3, vanillin stain). The organic solvent was removed *via* rotary evaporation and the resulting product was obtained as a transparent viscous liquid (yield = 54%).

¹H-NMR (300 MHz, Chloroform-d) δ 3.71 (s, 3H), 3.69 (s, 3H), 3.55 (m, 1H), 3.51 – 3.16 (m, 2H), 2.96 – 2.48 (m, 10H), 2.01 – 1.77 (m, 2H), 1.48 (s, 3H), 1.39 (s, 3H). **¹³C-NMR** (75 MHz, Chloroform-d) δ 173.16, 172.91, 157.90, 81.37, 64.50, 52.75 (d, J = 9.8 Hz), 42.31, 35.45, 32.27, 30.07, 29.41, 29.13, 28.36, 27.87, 22.55. **HRMS (ESI)** m/z: [M-Na]⁺ calcd for C₁₇H₃₀NO₆S₂, 430.1329; found, 430.1330

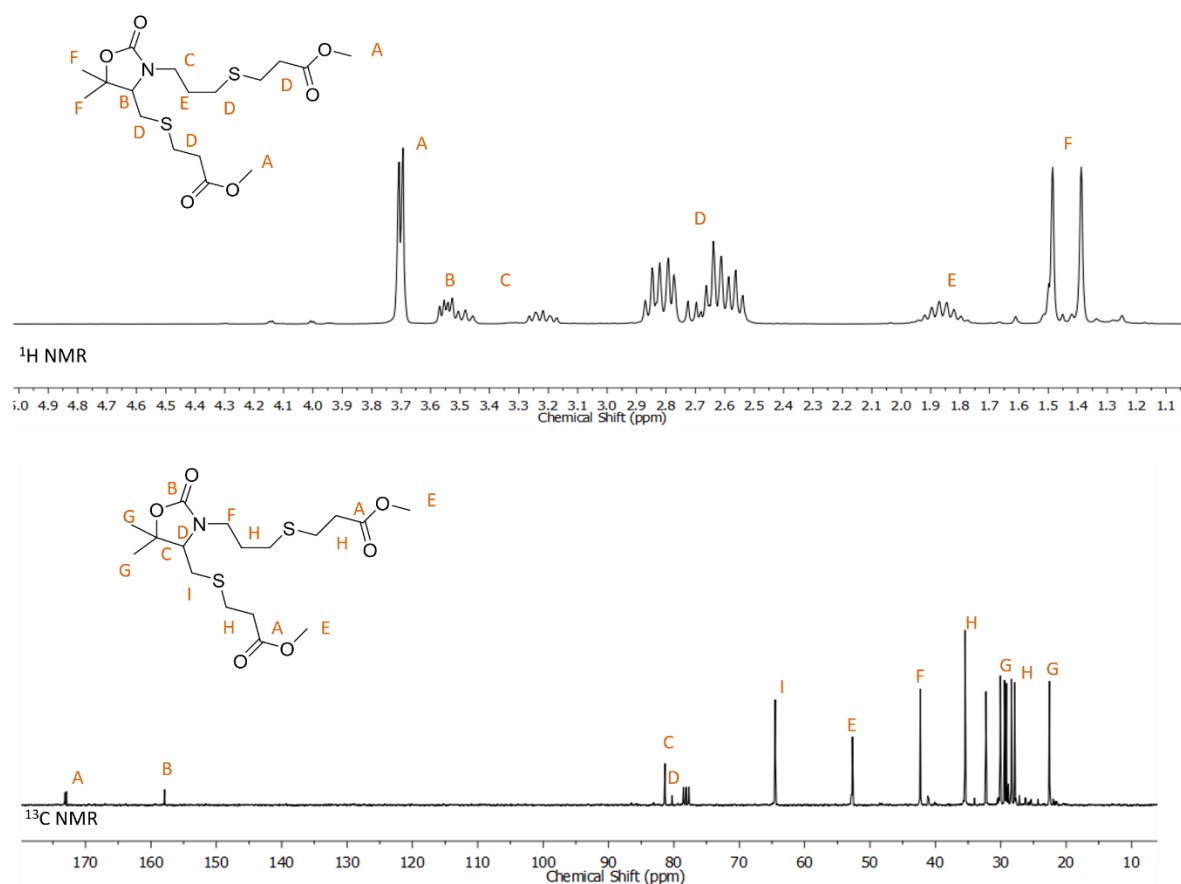


Figure S5. ¹H-NMR (top) and ¹³C-NMR (bottom) spectra of OX_S1 (CDCl₃)

S1.1.3 Synthesis Cationic model compounds OX_S2

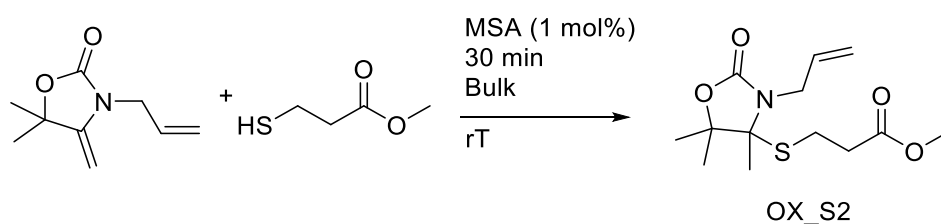


Figure S6. Synthesis of OX_S2

Allox (0.6 mmol, 1 eq) was mixed with methyl-3-mercaptopropionate (0.6 mmol, 1 eq) in a glass vial. MSA (1 mol%) was added to the mixture. The homogenous yellow mixture was stirred for 30 min. The resulting transparent mixture was diluted in EtOAc and was washed twice with subsaturated brine. The organic phases were dried over MgSO₄ and evaporated using rotary evaporation. The resulting yellow viscous liquid was subjected to column chromatography (Hex:EtOAc 8:2, vanillin and iodine stain). The organic solvent was removed *via* rotary evaporation and the resulting product was obtained as a transparent viscous liquid (yield = 74%).

¹H-NMR (300 MHz, DMSO-d₆) δ 6.01 – 5.81 (m, 1H), 5.35 – 5.02 (m, 2H), 3.85 (dddt, 2H), 3.61 (s, 3H), 2.86 – 2.33 (m, 4H), 1.55 (s, 3H), 1.40 (s, 3H), 1.34 (s, 3H). **¹³C-NMR** (75 MHz, DMSO) δ

171.50, 155.91, 134.34, 116.50, 85.38, 78.15, 51.55, 42.58, 40.33, 40.06, 39.78, 39.50, 39.22, 38.94, 38.66, 32.58, 24.92, 24.01, 23.01, 20.57 **HRMS (ESI)** m/z : $[M-H]^+$ calcd for $C_{17}H_{30}NO_6S_2H^+$, 288.3740; found, 288.3742

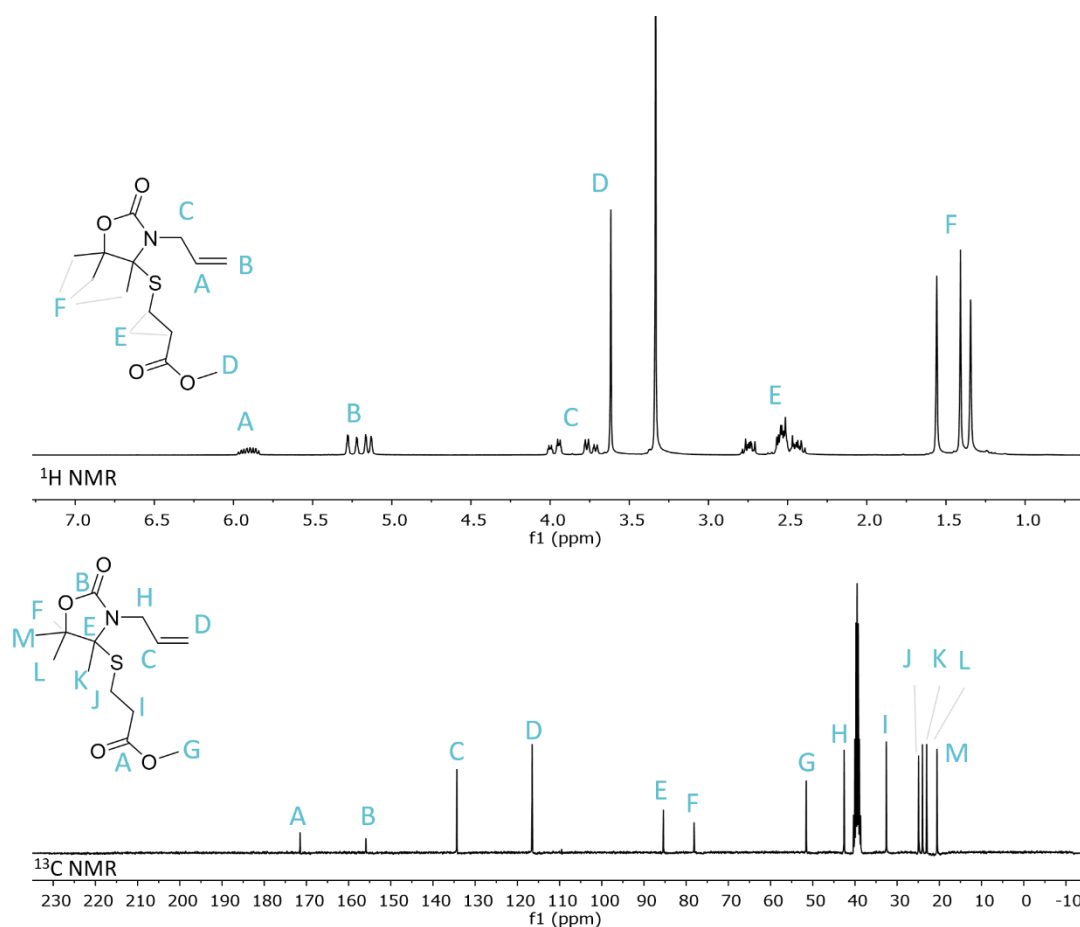


Figure S7. 1H -NMR (top) and ^{13}C -NMR (bottom) spectra of OX_S2 (DMSO- d_6)

1.1.2 Synthesis Tandem model compounds (OX_S3)

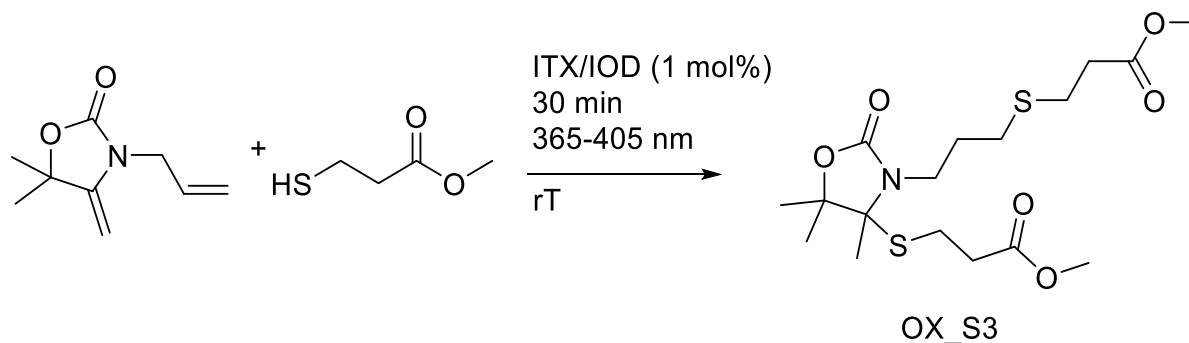


Figure S8. Synthesis of OX_S3

AlloX (0.6mmol, 1 eq) was mixed with methyl-3-mercaptopropionate (1.2 mmol, 2eq) in a glass vial. ITX and IOD (1 mol %) were added and the mixture was stirred until homogenous. The

yellow mixture was irradiated in an asiga flash curing chamber for 30 min under stirring (low pressure mercury lamp, 365-405 nm, 36 Watts). The resulting viscous yellow mixture was diluted in ethyl acetate and was washed twice with subsaturated brine. The organic phases were dried over MgSO₄ and evaporated using rotary evaporation. The resulting yellow viscous liquid was subjected to column chromatography (Hex:EtOAc 7:3, vanillin stain). The organic solvent was removed *via* rotary evaporation and the resulting product was obtained as a yellowish viscous liquid (yield = 74%)

¹H-NMR (300 MHz, Chloroform-d) δ 3.67 (s, 3H), 3.66 (s, 3H), 3.56 – 3.18 (m, 2H), 2.86 – 2.68 (m, 4H), 2.63 – 2.30 (m, 8H), 1.99 – 1.75 (m, 2H), 1.59 (s, 3H), 1.43 (s, 3H), 1.36 (s, 3H). **¹³C-NMR** (75 MHz, Chloroform-d) δ 172.26, 171.60, 157.20, 85.57, 79.33, 78.49, 51.89, 40.08, 34.56, 33.12, 29.48, 26.97, 25.33, 24.47, 23.42, 21.08. **HRMS (ESI)** m/z: [M-Na]⁺ calcd for C₁₇H₃₀NO₆S₂Na⁺, 430.1329; found, 430.1336

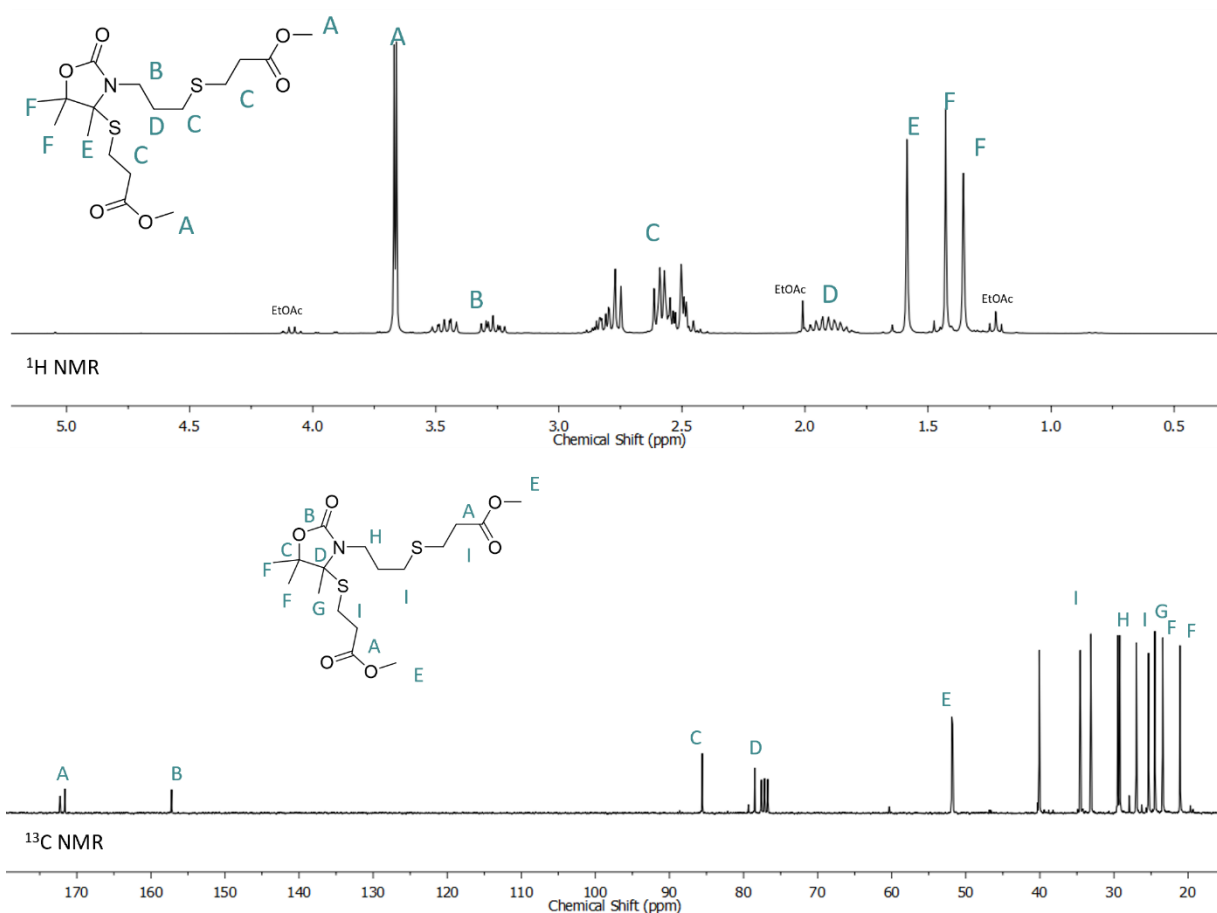


Figure S9. ¹H (top) and ¹³C-NMR (bottom) spectra of OX_S3 (CDCl₃)

S1.2 Methods

Nuclear magnetic resonance (NMR) spectroscopy. ¹H- and ¹³C-NMR analyses were performed on a Bruker Avance 300 MHz spectrometer at 25 °C in the Fourier transform mode using CDCl₃ or DMSO-*d*₆ as solvents.

SEC. The samples were first dried in an oven at 60 °C under vacuum and then redissolved in THF to achieve a concentration of about 1 mg·mL⁻¹. The solutions were filtered with a PTFE filter (pore size = 0.2 μm) before injection. The SEC (Agilent PL-GPC 50 integrated system) consisted of

an autosampler, a pump and a differential refractometer as detector. A guard column (Agilent PLGel 5 μ M, 50x1.5mm) and two columns (PLGel μ M, 30x7.5mm) were used for the fractionation at 40 °C using THF as eluent. The flow rate of THF through the columns was 1 mL·min⁻¹. The reported molar masses are referred to polystyrene standards and the data was processed with PL-GPC software control v.2.3.0 (Agilent).

HRMS (ESI) data were acquired in SCAN mode, using a mass range 50–1000 u in resolution mode (FWHM \approx 20,000) and a scan time of 0.1 s. The source temperature was set to 120 °C and the desolvation temperature to 350 °C. The capillary voltage was 0.7 kV and the cone voltage 15 V. Nitrogen was used as the desolvation and cone gas at flow rates of 600 L/h and 10 L/h, respectively. Before analysis, the mass spectrometer was calibrated with a sodium formate solution. A leucine-enkephalin solution was used for the lock mass correction, monitoring the ions at mass-to-charge ratio (m/z) 556.2771 and 278.1141. All of the acquired spectra were automatically corrected during acquisition based on the lock mass. The samples were dissolved in the corresponding solvent at a concentration of 1 mg/ml and diluted to 20 μ g/mL for the analysis.

Atom Economy Calculation Atom economy was calculated as described in². Briefly, Eq 1 was employed:

$$AE = \frac{Mass_{Product}}{\sum Mass_{Reactants}} * 100 \quad (1)$$

Gel content (GC). Films prepared as described in the experimental section were cut in rectangular shapes and weighted (m_1) before immersing 48 h in tetrahydrofuran. After weighing, the swelled films (m_2) were dried in a vacuum oven at 60 °C for 24 h. The films were weighed once again (m_3). Swelling (SI) and Gel content (GC) were calculated with equation 2 and 3, respectively:

$$SI = 100 * \frac{m_2}{m_1} \quad (2)$$

$$GC = 100 * \frac{m_3}{m_1} \quad (3)$$

Tensile tests were carried out on dogbone samples (see Preparation of Films below) (ASTM D638 TYPE V) in an Instron 5569 tensile tester (Instron, Norwood, MA, USA). Young's modulus, Tensile strength (σ_t), Yield strength (σ_y), and strain at break (ϵ_b) were determined using Bluehill software from the load-displacement curves at a crosshead speed of 10 mm/min. A minimum of three tensile specimens were tested for each reported value. Cyclic tensile tests were conducted to 20% strain at a rate of 10 mm min⁻¹. 10 Cycles were measured. Calculation of elastic recovery was carried out following previous works.³

Finite Element Digital Image Correlation (FE-DIC) To efficiently measure and discriminate the differences between the upper (soft) part and lower (rigid) part of the locally heat-treated dogbone sample, full field strain measurements were performed. Indeed, direct measurements from the tensile testing apparatus will lead to mistake in the strain value due to the assumption of a homogeneous

material, which is not anymore the case. Digital image correlation (DIC) allows to compute globally the strain field of a sample and thus differences can be observed compared to a general extensometer measurements. A Baumer® Vexu-24M camera was used with an in-house python software to record images at a 2 Hz frequency. A white and black speckle pattern was laid on specimen with a spray-paint. A white layer was firstly spread on the sample, black paint was then projected to generate random pattern composed of black dots. Images were post-processed with Pyxel,⁴ a finite-element DIC Python software developed at the Clément Ader Institute (Toulouse, France). This method relies on minimising distance between two functions linked to reference and deformed images respectively by analysing grey level of finite element's degree of freedom (dof) environment. Since the displacement obtained for each dof is linked to a finite element mesh, deformation field can be obtained by derivation using a Gauss-Newton algorithm.⁵ The Region of Interest (ROI) was set for the global sample to 20 mm x 3 mm window placed in the narrower area of the sample. Finite-Element Mesh is composed of 50 elements of 0.6 mm x 2 mm size each with 8 dofs per element. To also compute and compare completely the upper and lower part of the sample, two different ROI were used, localized manually on the respective upper and lower part of the sample (CF IMAGES (if needed)). The ROI was set at 3 x 10 mm with 25 elements 0.2 x 2 mm size elements. In order to avoid computational costs and divergences at high displacement, the DIC measurements were only performed up to 10 % strain.

Fourier Transform Infrared Spectroscopy (FT-IR) spectra were recorded on a Nicolet iS20 Spectrometer using Attenuated Total Reflection (ATR) at a resolution of 4 cm⁻¹ and a total of 32 interferograms. Kinetics were recorded on the same instrument averaging 4 interferograms per spectra at the same resolution. The spectra at high temperature were obtained on a Nicolet 6700FT-IR spectrophotometer equipped with a specap variable temperature transmission cell. Spectra were recorded in the range of 4000 and 400 cm⁻¹ with a spectrum resolution of 4 cm⁻¹, and a total of 64 interferograms. Samples were prepared by photocuring the resins composed of equimolar amounts of AlLOx, S4 and photoinitiator system (0.5 wt%) on KBr windows. The spectra were then acquired at each temperature after 5 min of equilibration. To calculate the amount of adduct at a given temperature the peak at 1678 cm⁻¹ was integrated. Conversion was calculated assuming that the integral of the peak at 175 °C was 83% of dissociation (from ¹H NMR experiments) using eq 4:

$$\text{Estimated Adduct bulk material (\%)} = \frac{\text{Area}_{\text{Temperature}}}{\text{Area}_{100\% \text{ adduct}}} * 100 \quad (4)$$

Modulated Differential Scanning Calorimetry was performed on a TA Instruments DSC 250 calibrated with indium, and the curves were analyzed using the Trios software. A period of 60 seconds with an amplitude of 1 °C was used. A ramp of 3 °C per minute from -20 °C to 175 °C.

Dynamic Mechanical Analysis (DMA) was performed on a DMA Q800. A 10 mm x 2 mm x 0.7 mm (l x w x t) was placed in a tension film clamp. An oscillation amplitude of 15 µm and a static force of 0.01 N were employed. A ramp of 3 °C/min was used from -20 to 175 with a frequency of 1 Hz. T_α was measured as the peak in the Tan delta curve.

Isothermal stress relaxation was conducted on a DMAQ800 in tension mode. Rectangular samples of 15×6×0.5 mm were used. The sample was held at the desired temperature for 10 min before a 1% strain was applied. The strain was kept constant for 60 min. Stress–relaxation of the dynamic

cross-linked network was defined using a first order Maxwell model (Equation 4). The Flow Activation Energy (E_{flow}) was then extracted by plotting an Arrhenius relationship (Equation 5) with τ^* as a function of $1/T$ (eq).

$$\frac{G(t)}{G_0} = e^{-t/\tau^*} \quad (5)$$

$$\tau^* = \tau_0 e^{E_a/RT} \quad (6)$$

TEM was acquired on a TECNAI G2 20 TWIN FEI transmission electron microscope equipped with LaB6 filament operated at an accelerating voltage of 120 kV in bright-field image mode at magnifications between $\times 6500$ and $\times 50k$. The samples were about 80 nm thick and were obtained by cutting at -90°C using a Leica EMFC6 cryoultramicrotome device equipped with a diamond knife. These ultrathin sections were placed on a 300 mesh-formvar Cu grids for imaging. No staining was carried out.

AFM was acquired in tapping mode using a Dimension ICON (Bruker) with Nanoscope VI (Bruker) as software. A TESP-V2 cantilever was used at 320 kHz frequency (Spring constant: 37 N/m, radius 7 nm, length 125 μm , silicon, repulsive mode, 25°C). Images were elaborated using Nanoscope Software. A first order background was removed, and the images were coloured with the standard colour palette. To compare images of different materials the same scale was used. The Nanoscope plugin “particle analysis” was used to estimate size and area % of the hard phase.

Nano-FTIR and s-NOM were recorded with a neaSNOM system (Neaspec GmbH, Germany) comprising both s-SNOM and nano-FTIR capabilities. Pt-Si coated AFM tips were used. IR s-SNOM imaging was performed with illumination from a tunable quantum cascade laser. Nano-FTIR spectroscopy was performed with illumination from amid-infrared laser supercontinuum. The final nano-FTIR spectra were obtained by averaging 25 individual spectra. The total acquisition time was 15 min and the spectral resolution 17 cm^{-1} . The spectra were normalized to that obtained on a clean gold surface (reference measurements). Data were analyzed using Gwyddion.

Temperature Sweep Rheology was performed on an Ares G2 rheometer with a 12 mm plate-plate geometry. A ramp of $3^\circ\text{C}/\text{min}$ was used with a 1% strain and 0.5 Hz frequency. A 0.2 N normal force was applied to the material before starting to measurement to ensure good contact with the plates.

Frequency Sweep Rheology was performed on an Ares G2 rheometer with a 12 mm plate-plate geometry. A 5% strain was applied after isothermal for 10 min at the desired temperature. Then a frequency sweep from 0.01 to 100 Hz was performed. A 0.2 N normal force was applied to the material before starting to measurement to ensure good contact with the plates.

Photorheology was performed on an ARG2. A LED UV-curing accessory centered at 365 nm (20 mW/cm²) was used together with an acrylic transparent bottom plate and a single use aluminum

parallel plate (20 mm). The measurement was performed in the linear viscoelastic regimen with frequency of 1 Hz with a gap of 400 μm .

Optical Microscopy and Confocal raman Raman spectra were collected using a Witec alpha300RA equipment. An excitation wavelengths of 785 nm was used with typical integration time per point of around 500 ms and 50 accumulations. Reported data correspond to average values after removing cosmic ray artifacts. A 100x objective was used for confocal measurements. Additionally, Raman images were taken over sample areas of about 100 micrometers squared with data points measured every 200 nm.

Radical, Tandem and Cationic Model Reactions

Model reactions between AlLOx and 3-methyl mercaptopropionate were carried out with 3 different initiators. The two components were mixed in equal SH to double bond ratio in bulk with the photoinitiator. The samples were irradiated at 390nm (20 mW/cm²) and aliquots of the reaction mixture were sampled over time. The reactions were monitored by ¹H-NMR spectroscopy to determine the conversion in the product.

For all reaction the conversion was calculated with Equation 7 (where I_t is the integral at time t and I_0 the integral at time 0) by taking into consideration the signal of the CH₂ of the allyl bond (5.16 ppm), CH₂ of exovinylene double bond (3.98 ppm). The signal were normalized using the signal of the internal standard (1,3,5-trimethoxy benzene, signal at 6.06 ppm, singlet). For the cationic thiol ene kinetics the signal of the methyl of 3MP was used as internal standard (3.68 ppm, singlet)

$$\text{Conversion (\%)} = \frac{I_t}{I_0} * 100 \quad (7)$$

Radical Model Reaction: AlLOx (4 mmol, 1 eq.), 1,3,5-trimethoxy benzene (10 mg) and 3-methyl mercaptopropionate (8 mmol, 2 eq.) were added to a vial. ITX (1 mol%) was added and the mixture was stirred until complete dissolution. The mixture was then irradiated with a 390 nm light (Kessil, PR160L, 390nm, 20 mW/cm²). The NMR sample were prepared by dissolving 10 μL of the reaction medium in 500 μL CDCl₃ and were stored in the dark before measurement.

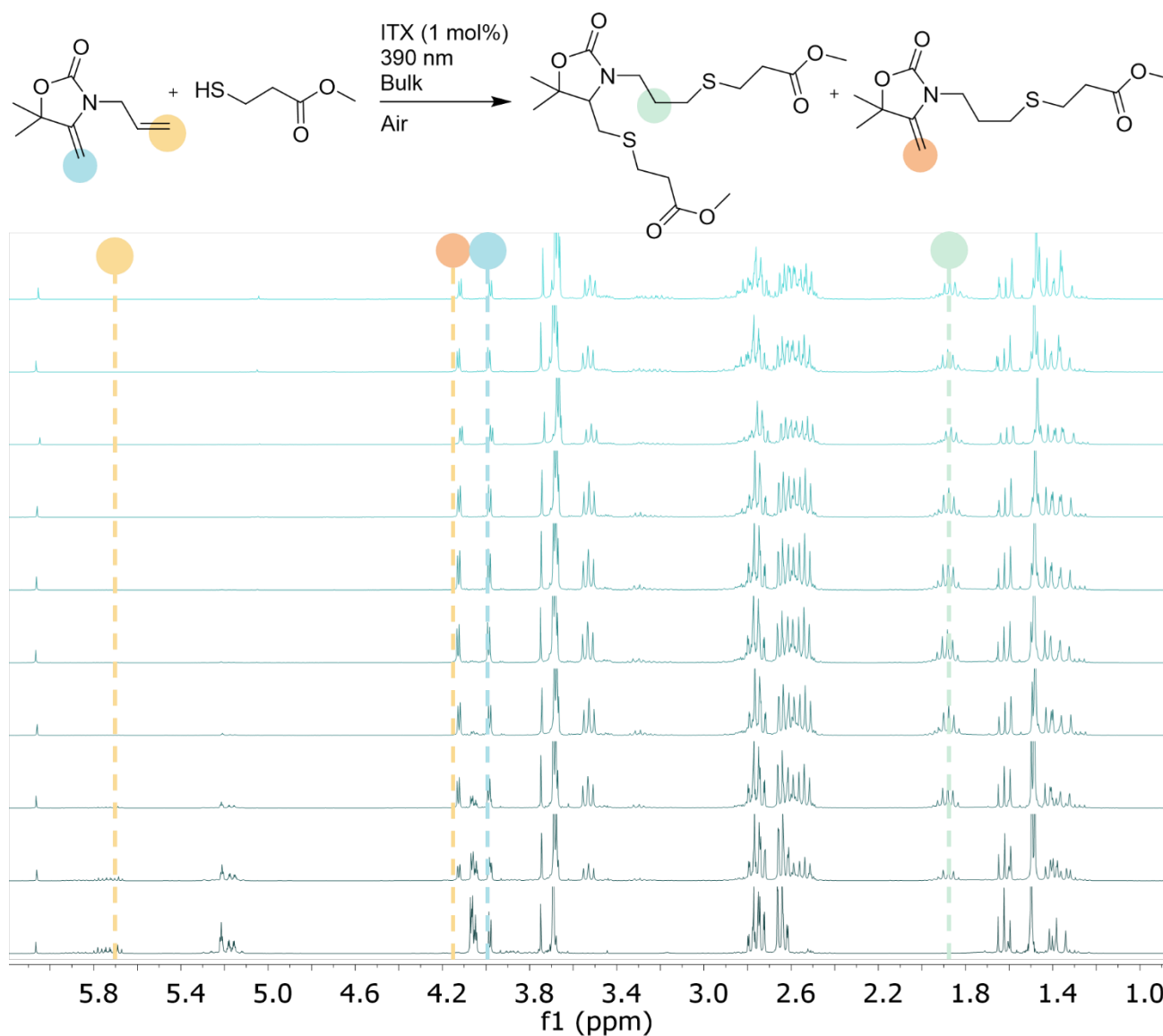


Figure S10. ^1H NMR kinetics of model radical thiol ene using ITX as photoinitiator

Radical Model Reaction: AlIOx (4 mmol, 1 eq.), 1,3,5-trimethoxy benzene (10 mg) and 3-methyl mercaptopropionate (8 mmol, 2 eq.) were added to a vial. BAPO (1 mol%) was added and the mixture was stirred until complete dissolution. The mixture was then irradiated with a 390 nm light (Kessil, PR160L, 390nm, 20 mW/cm²). The NMR sample were prepared by dissolving 10 μL of the reaction medium in 500 μL CDCl_3 and were stored in the dark before measurement.

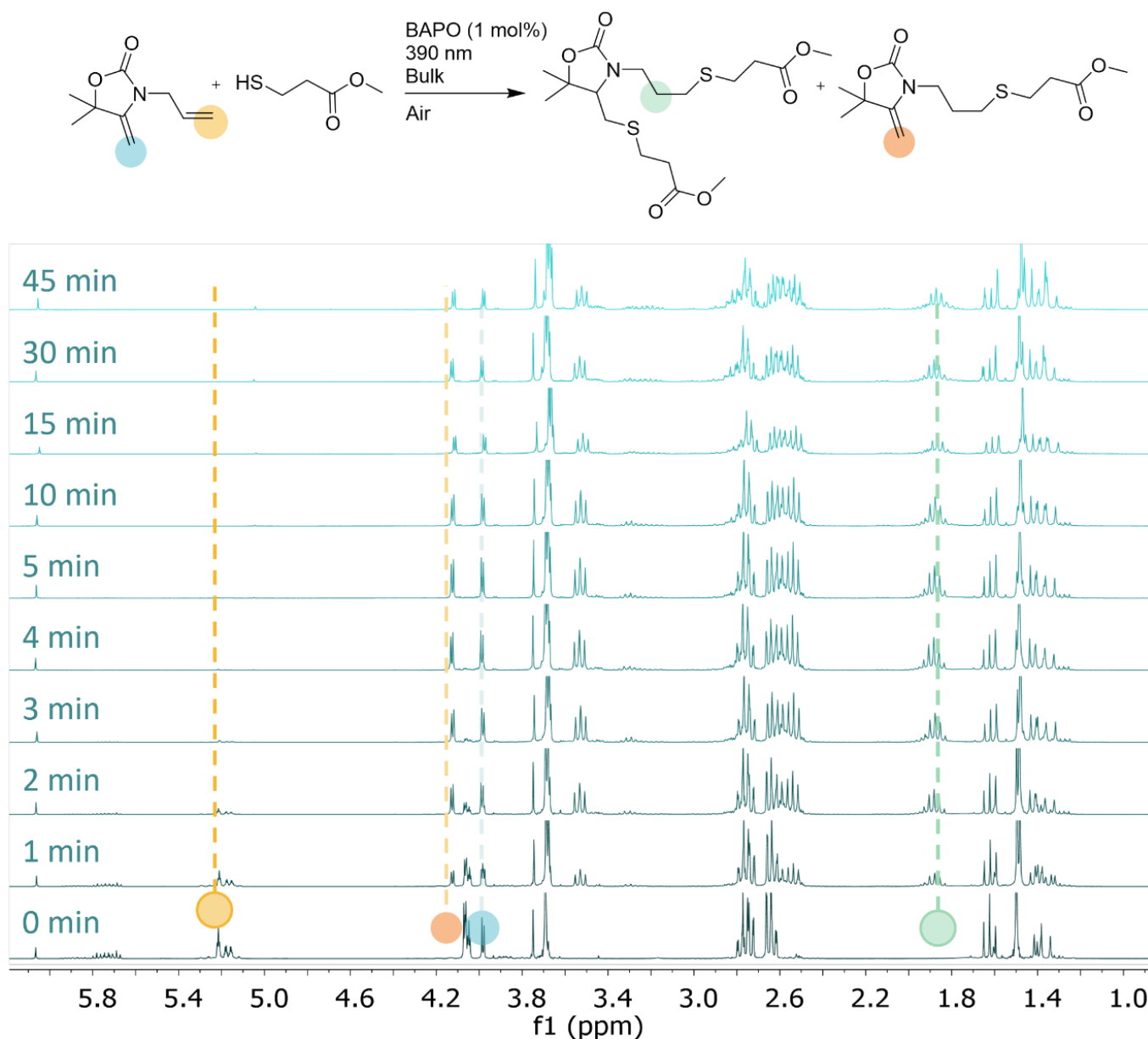


Figure S11. ¹H NMR kinetics of model radical thiol-ene using BAPO as photoinitiator

Cationic Model Reaction: AlloX (4 mmol, 1 eq) and 3-methyl mercaptopropionate (8 mmol, 2 eq.) were added to a vial. MSA (1 mol%) was added. The NMR samples were prepared by quenching 10 μ L of the reaction medium in 500 μ L of CDCl₃ with 5 μ L of Triethylamine.

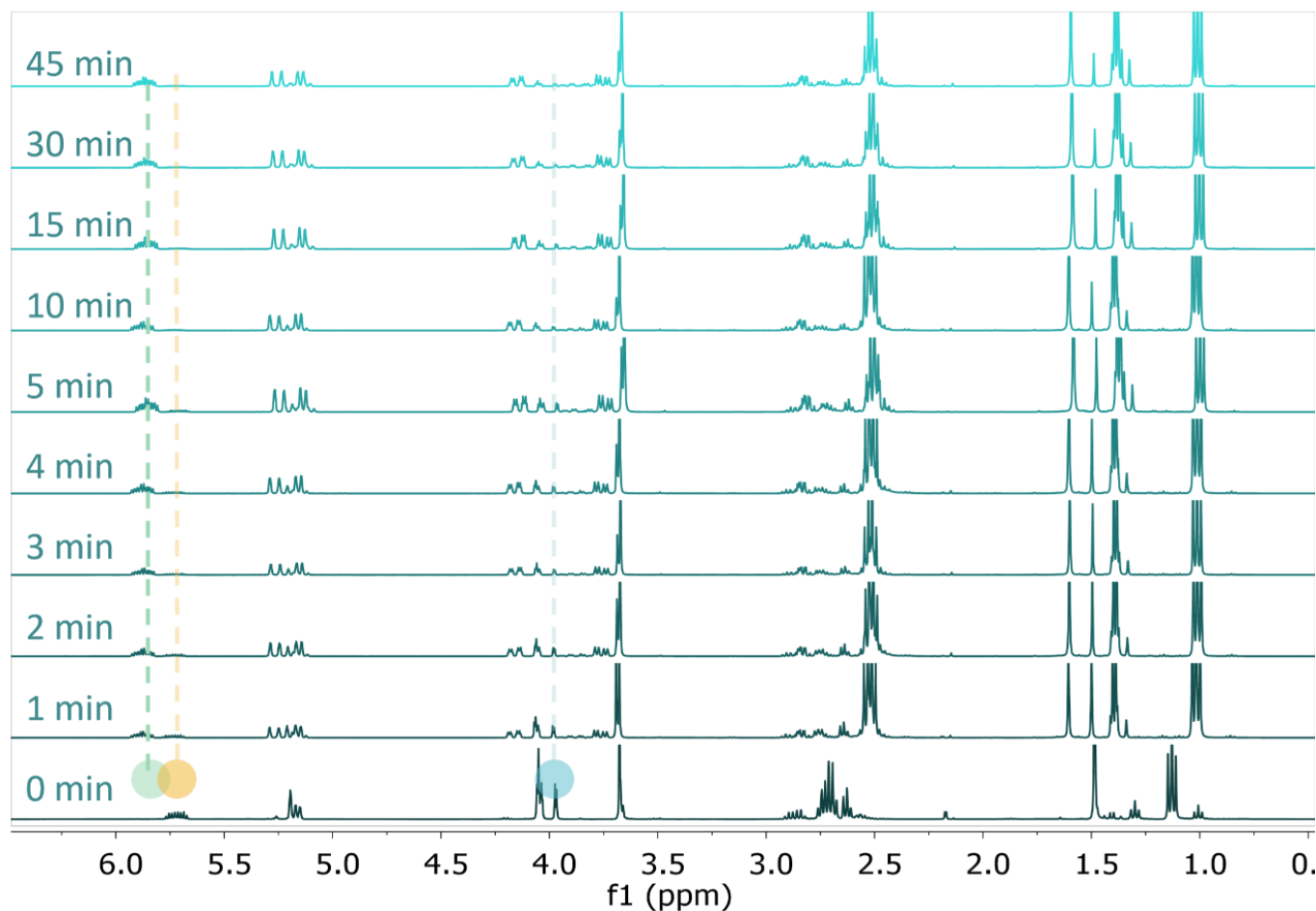
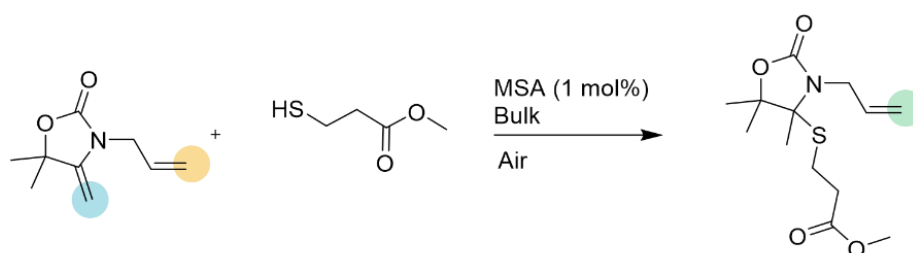


Figure S12. ¹H NMR kinetics of model cationic thiol ene

Tandem Model Reaction: AlloX (4 mmol, 1 eq.), 1,3,5-trimethoxy benzene (10 mg) and 3-methyl mercaptopropionate (8 mmol, 2 eq.) were added to a vial. IOD/ITX (1 mol% of each component) was added and the mixture was stirred until complete dissolution. The mixture was then irradiated with a 390 nm light (Kessil, PR160L, 390nm, 20 mW/cm²). The NMR sample were prepared by dissolving 10 μ L of the reaction medium in 500 μ L CDCl₃ with 5 μ L of Triethylamine and were stored in the dark before measurement.

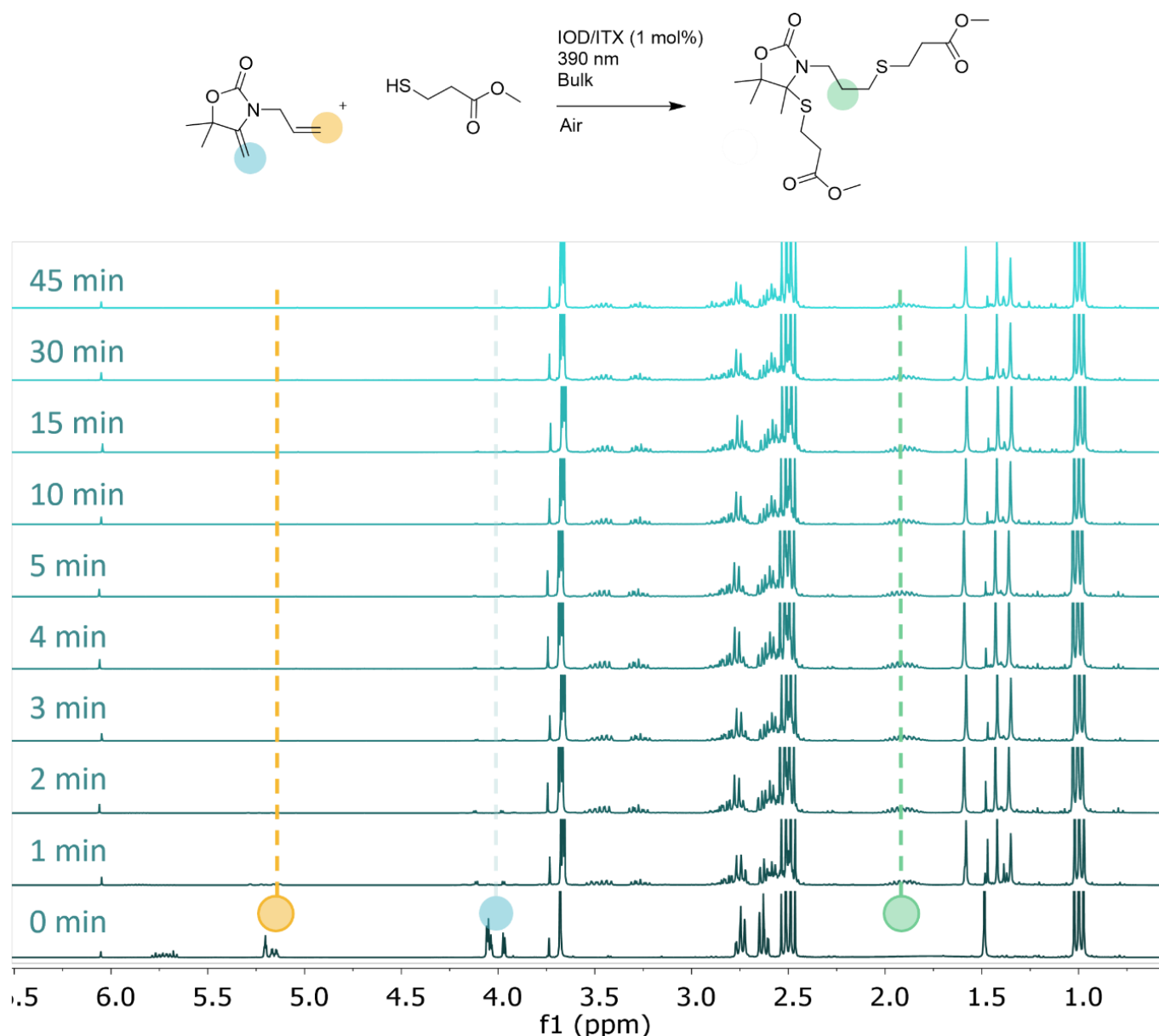


Figure S13. ^1H NMR kinetics of model tandem thiol-ene

Preparation of Crosslinked Networks and Films

The photoinitiators were first dissolved in AlLOx (0.5 wt%). The mixture was mixed with a vortex mixer for 30 s before adding the crosslinker (equimolar amount of SH to double bond functionality). As an example, T_S4 was prepared by mixing IOD/ITX (12.5 mg, 0.5 wt%) in AlLOx (1 g, 6 mmol, 2 eq), to which S4 (1.5 g, 3 mmol, 1 eq) were added via pipette. Other networks were prepared in an analogous manner. The resulting mixture was again vortexed for 1 min. The liquid was then poured into molds and cured for 30 min in an Asiga post-cure chamber (Low pressure mercury lamp with a broad emission in the UV and visible). For the various heat treatments, films were placed in a temperature control oven at the desired temperature for 16-20 hours, then cooled quickly to room temperature, and finally stored for 24 h at room temperature before testing their properties. The materials are named R_Sn for radical materials and T_Sn for tandem materials with n being the number of functionality of the thiol crosslinked used.

Films with spatially-resolved annealing were prepared by first treating the entire dogbone at 60 °C for 24 h. Then half of the dogbone was placed on a hot plate at 110 °C for 4 h to erase the phase separated structure.

Reprocessing of Films

The material was grinded and then hot-pressed in a Collin P200E hydraulic press for 3 min at 100 °C with an applied pressure of 10 tons. The resulting film was cooled down for 10 min before cutting dogbone samples (ASTM D638 TYPE V) with a die cutter. The resulting dogbone shapes were heat treated 24 h, cooled quickly to room temperature and then stored for 24 h at room temperature before testing.

Preparation of Films for AFM analysis

The photoinitiator system was first dissolved in AlIOx (0.5 wt%). The mixture was mixed with a vortex mixer for 30 s before adding the crosslinker (equimolar amount of SH to double bond functionality). The resulting mixture was again vortexed for 1 min. The resin was then brought into a Glovebox to avoid dust contamination (Argon atmosphere). The liquid was then drop casted on a glass slide and cured for 5 min with a 365 nm lamp at 20 mW/cm². The cured films were placed in an airtight container under normal atmosphere before being heat treated and then cooled quickly to room temperature. The samples were stored for 24 h at room temperature in a desiccator before testing their properties.

3D Printing

The material was grinded and then extruded through a twin-screw extruder at The filament was extruded using a twin screw extruder at 165 °C and 30 rpm to obtain a homogenous filament. The filament was let to rest for 30 min at room temperature and then cut into pellets using a pelletizer. The resulting pellets were stored in a desiccator to avoid any humidity absorption. They were then charged in an Ender 3 NEO retrofitted with a V4 Pellet extruder and a 0.4 mm nozzle. The nozzle was set at 185 °C and a speed of 5 mm/s was employed. Layers of 0.2 mm were printed. A skirt of 6 lines was used to reach a stable filament deposition.

After optimization it was found that a low speed and a more pronounced thermal gradient were necessary to fully depolymerize the polymer as the melting was given by a chemical reaction. Hence slow printing speed, coupled with a fan that is located further away from the nozzle helped with the deposition of a homogenous filament. A consistent size of pellets was also fundamental in having consistent material flow.

S2 Photocuring and Materials Properties

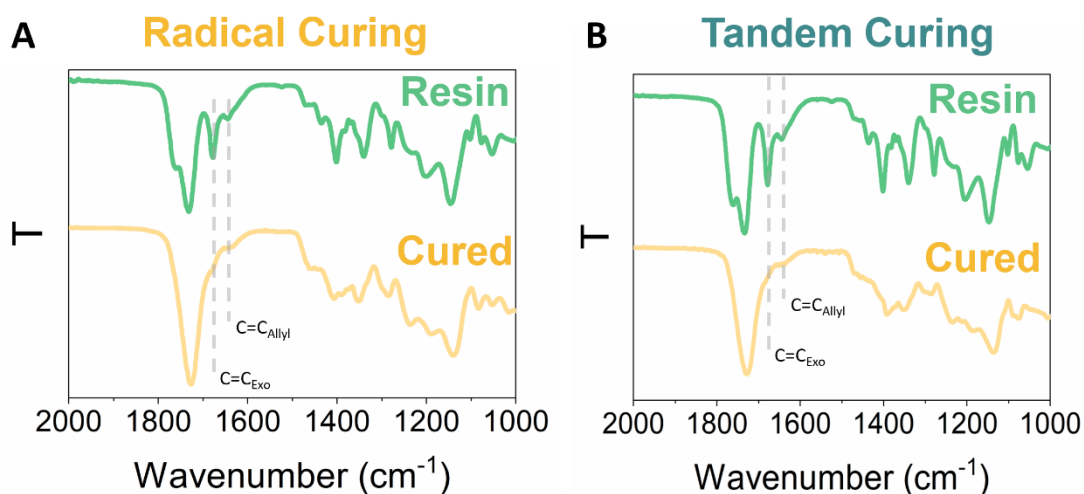


Figure S14. IR spectra of the resin and photocured radical material (Radical_S4) (b) IR spectra of the resin and photocured tandem material (Tandem_S4). The thiol band was not used to estimate the conversion as its signal to noise ratio was unsatisfactory.

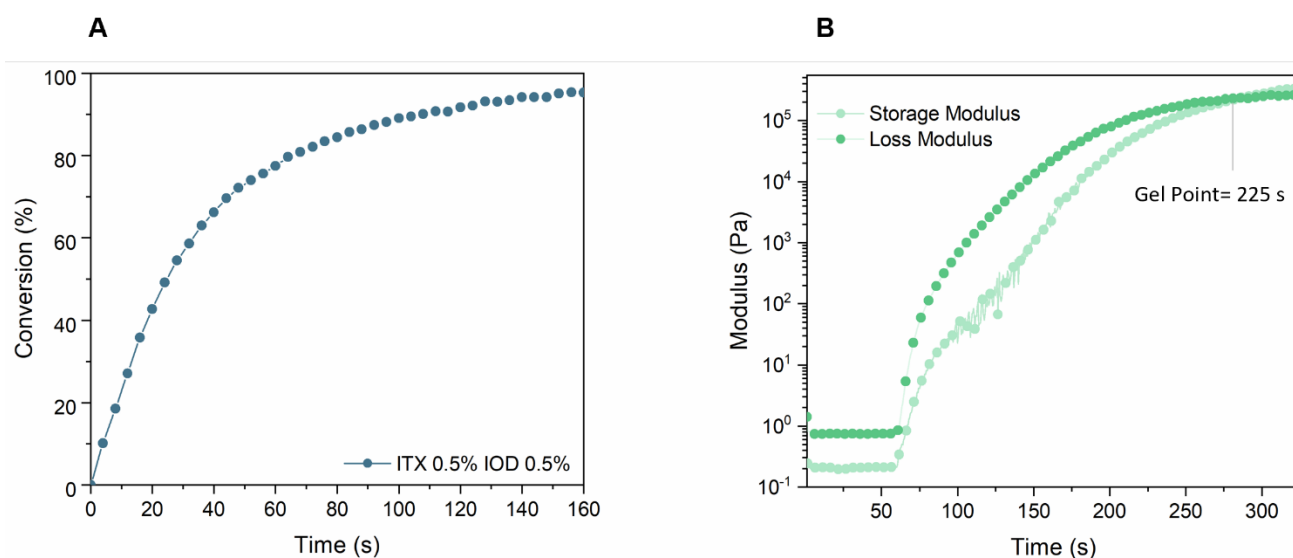


Figure S15. Conversion over time as calculated by RT FTIR analysis (a) Photorheology of T_S4 (b)

Table S1 Gel Content and Swelling in THF of Tandem and radical material

PI	Crosslinker	SI (THF)	GC (THF)
Tandem	S4	156±4	95±3
Radical	S4	146±0.5	98±0.3

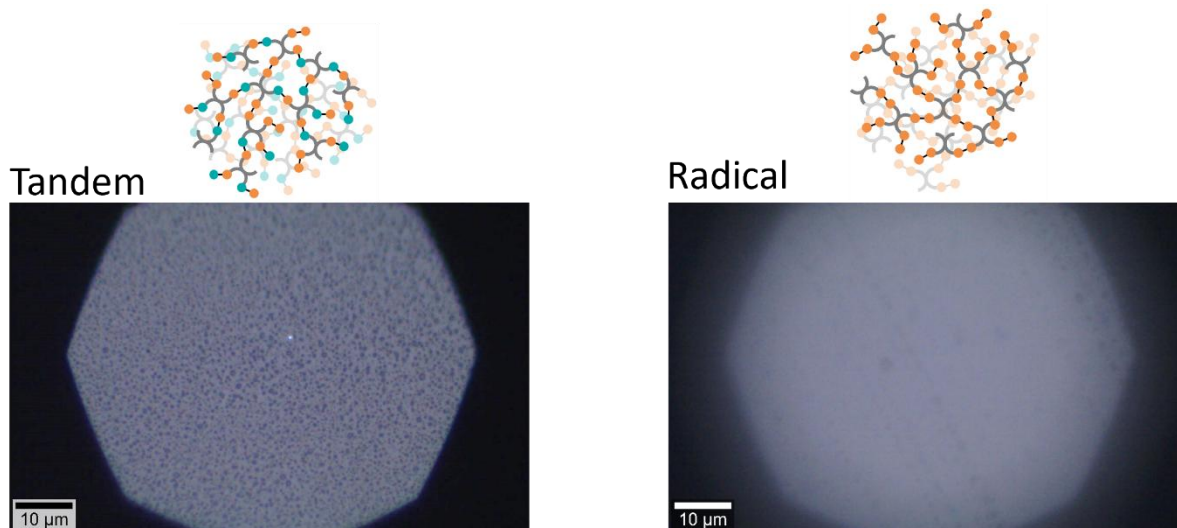


Figure S16. OM of Tandem material (T_S4) and Radical material (R_S4)

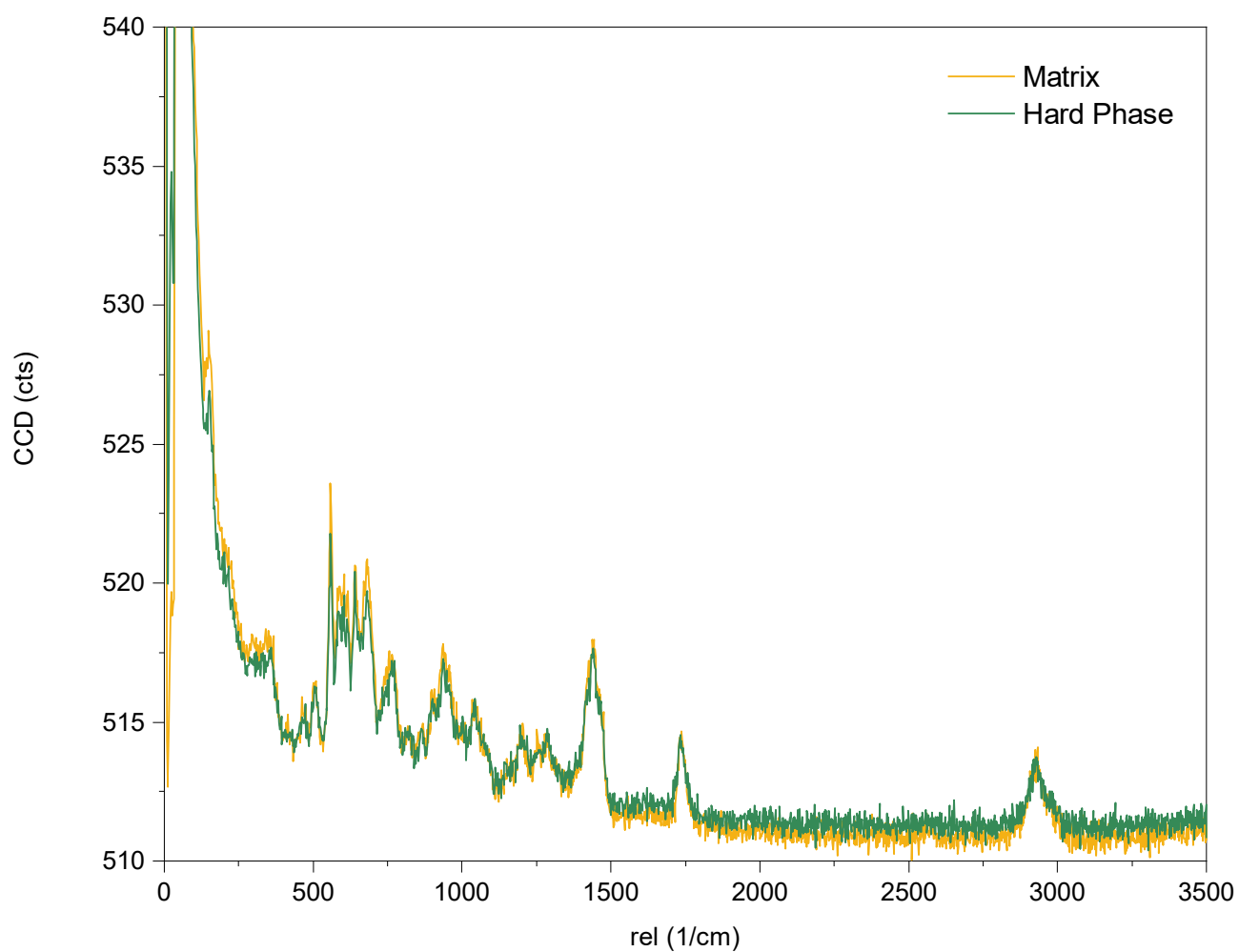


Figure S17. Confocal Raman spectra of hard phase and matrix of T_S4

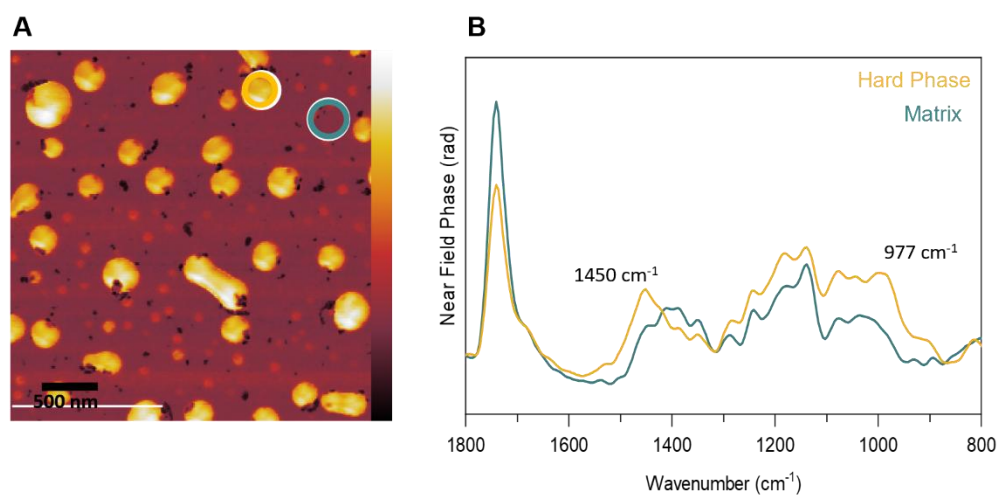


Figure S18. AFM Phase Imaging of T_S4 and corresponding Nano-FTIR spectra of the hard phase and matrix

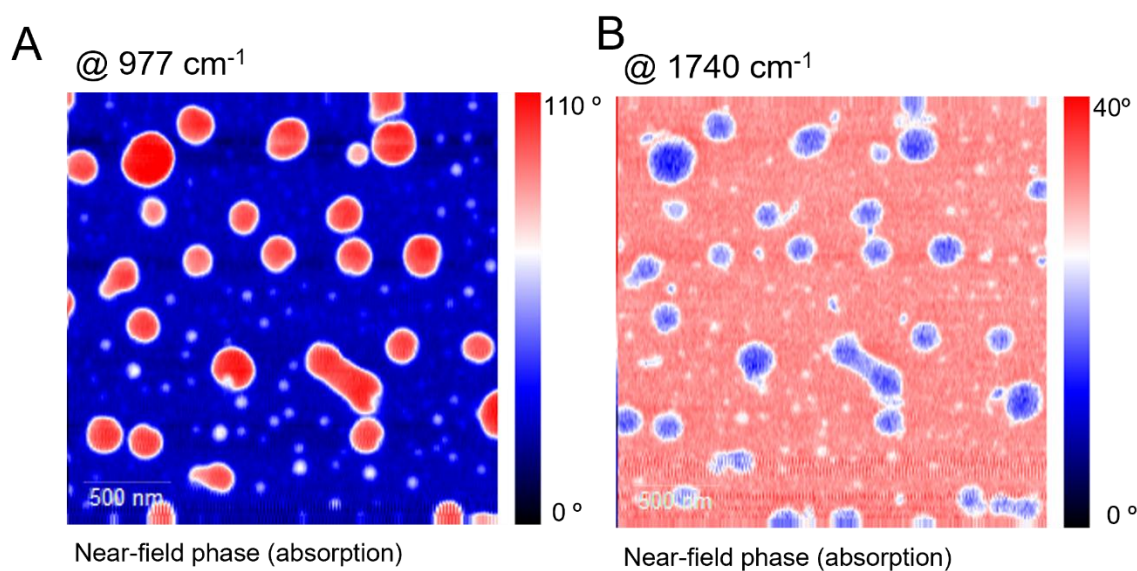


Figure S19. s-NOM imaging at 977 cm^{-1} (A) and 1741 cm^{-1} (B) of the tandem material (T_S4)

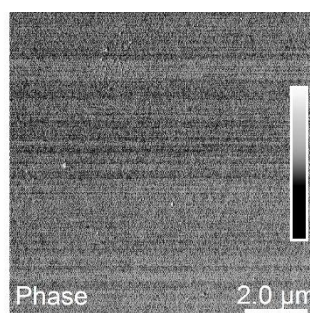


Figure S20. AFM of R_S4

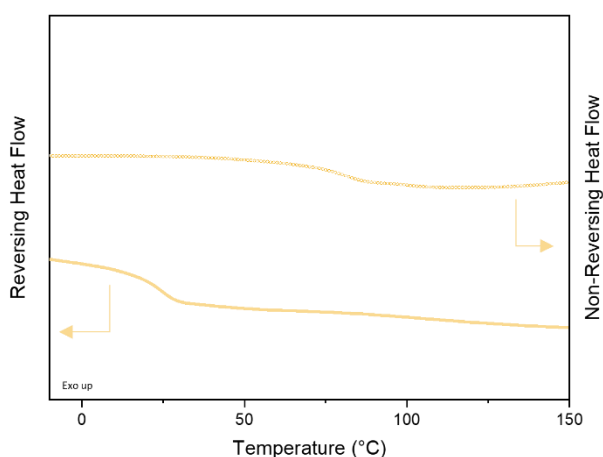


Figure S21. mDSC of radical material (R_S4)

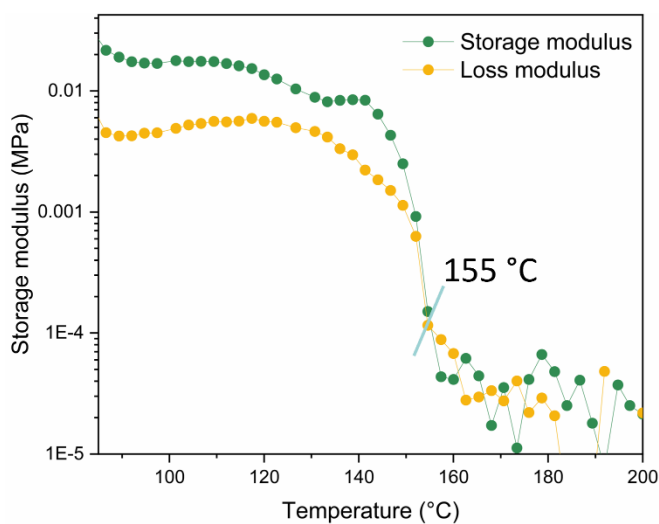


Figure S22. Temperature Sweep of Tandem_S4

Estimation of Adduct Dissociation

Ox_S3 was mixed with MSA (1 mol%) and placed in a vial under N₂ atmosphere. The mixture was heated at the desired temperature for 15 min, a small aliquot (1 uL) was then sampled and quenched with TEA (2 uL). The mixture was diluted in DMSO-*d*₆ (0.5 mL) and its ¹H NMR recorded. The conversion was estimated by the disappearance of the methyl signals of OX_S3 (1.59 ppm) using Equation 5.

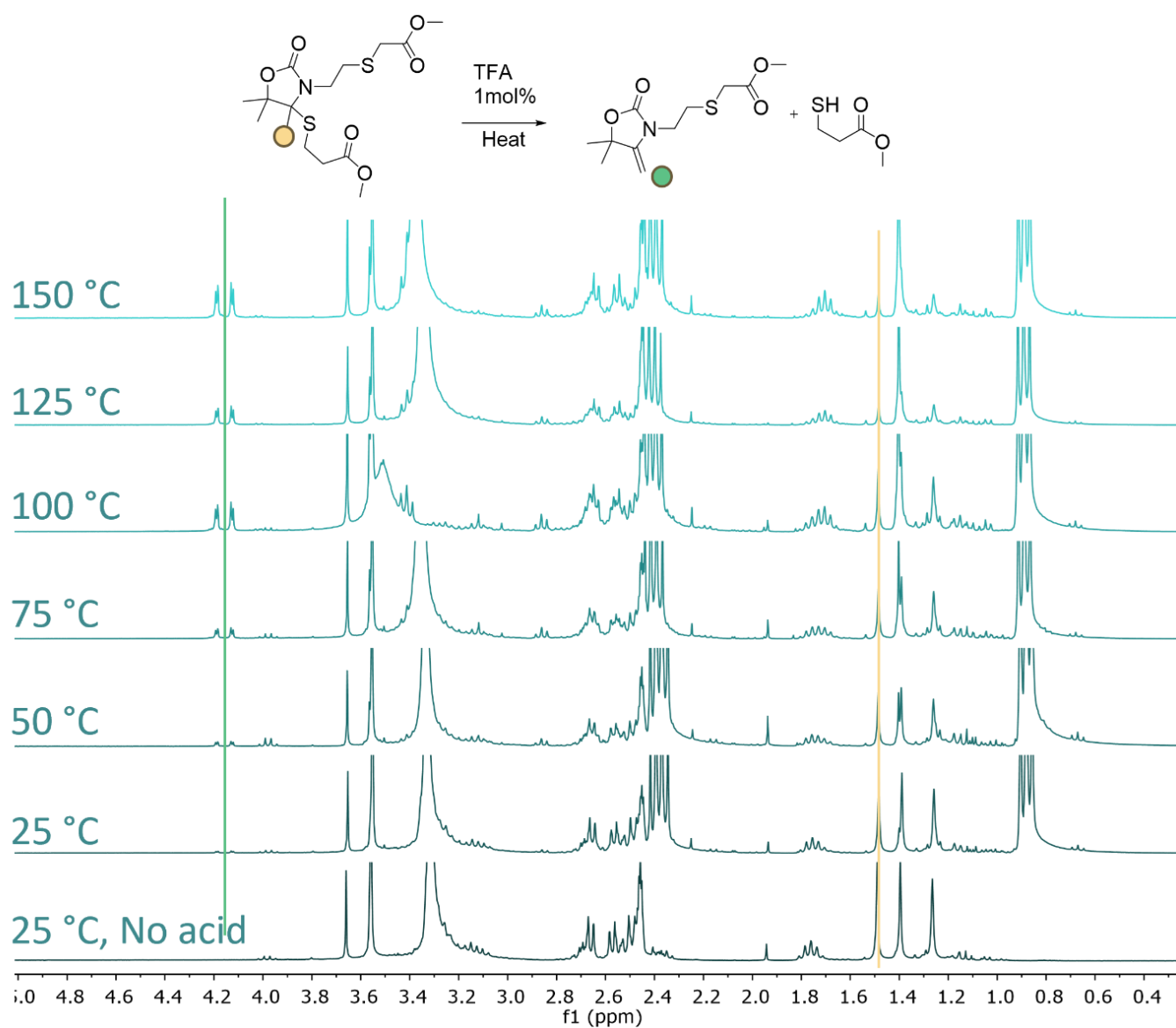


Figure S23. ^1H NMR experiment of *Adduct Dissociation* (Ox_S3) at different temperatures (DMSO d_6)

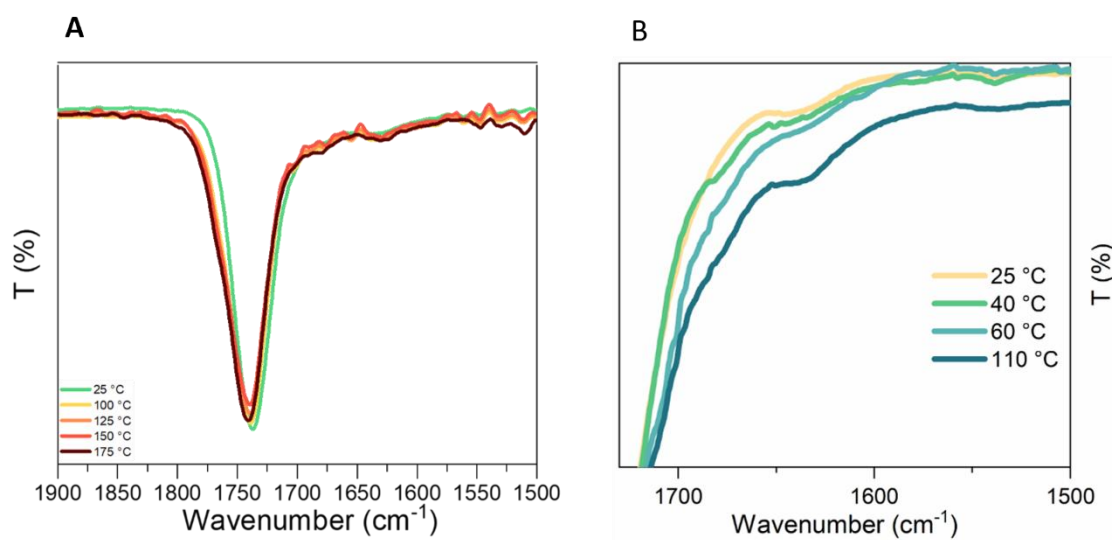


Figure S24. Temperature Dependent IR spectroscopy of Radical material (**R_S4**, a) and spectra of **T_S4** after thermal treatment (b)

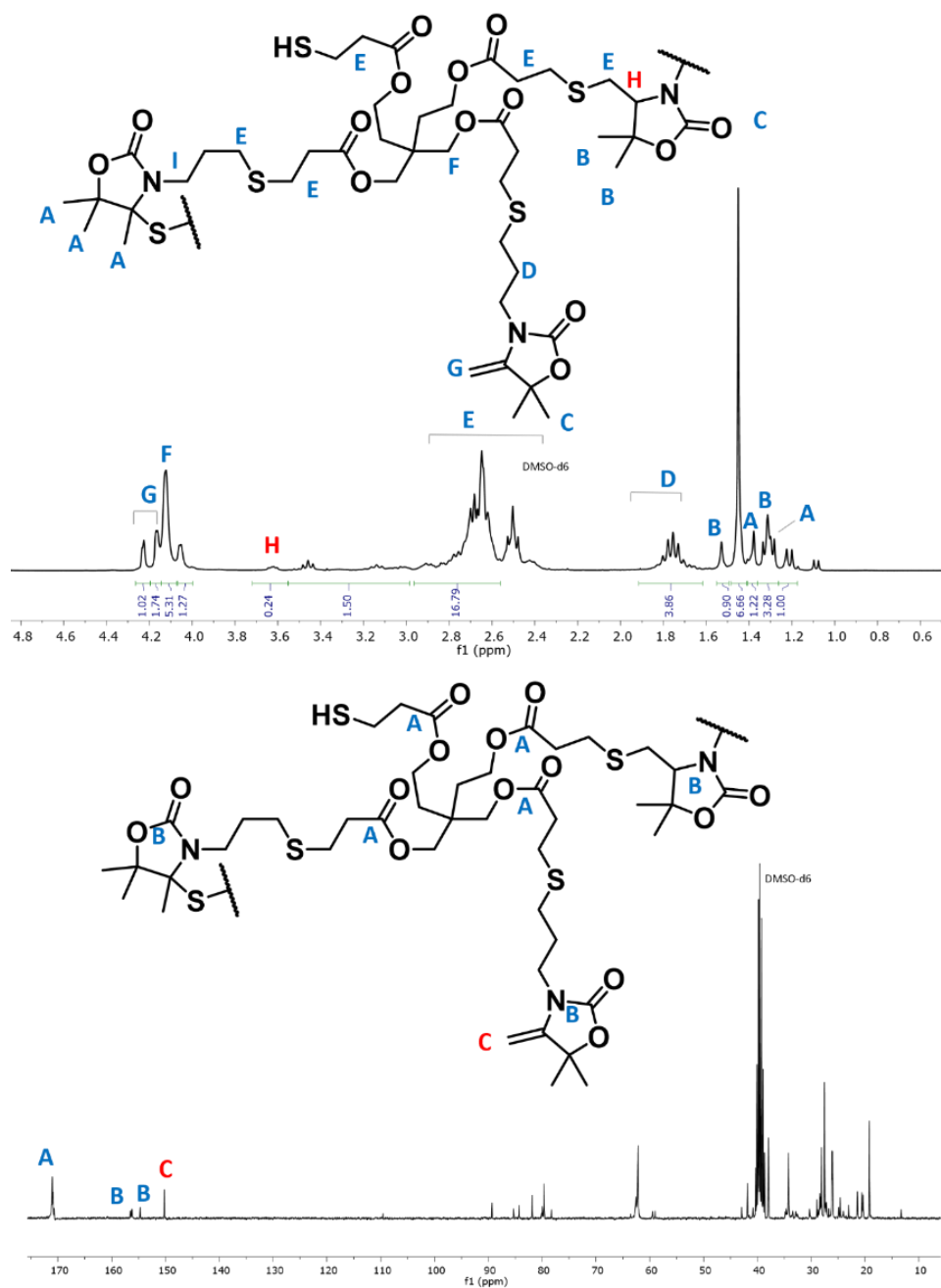


Figure S25. ^1H - (top) and ^{13}C -NMR (bottom) spectra of the depolymerised tandem material (Tandem_S4). AlloX was used as a model compound to assign signals C, G while the tandem and radical compound (OX_S1) helped for resonances A, D and H (^1H).

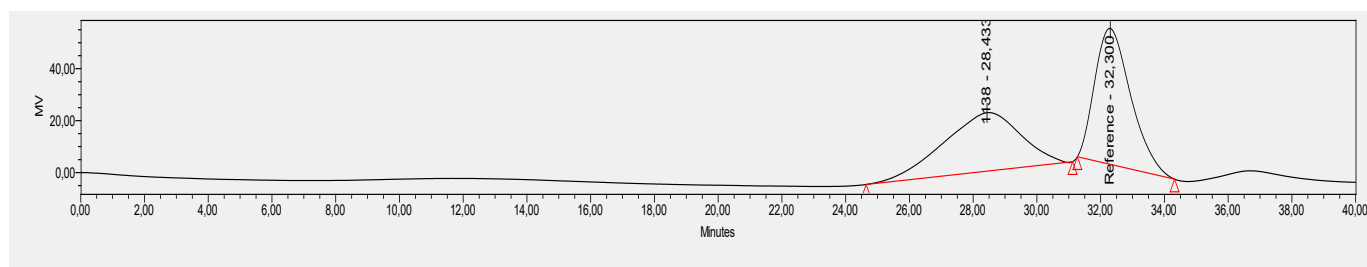
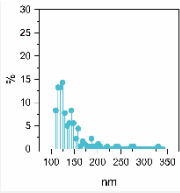
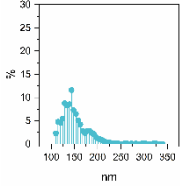
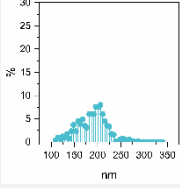
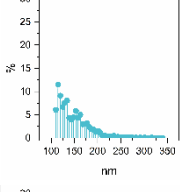
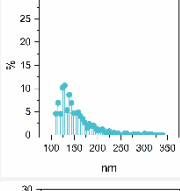
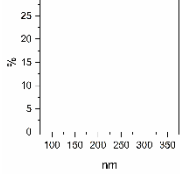


Figure S26. SEC trace of T_S4 after thermal depolymerisation

S3 Phase Separation

Table S2 AFM Characterisation of Hard phase in Tandem_S4 with different heat treatments

Heat treatment	Particle Distribution	Mean Particle size (nm)	Area Hard Phase
25 °C		84±25	1.4 %
40 °C		152±92	5.8 %
60 °C		168±51	25.6 %
75 °C		118±18	16.4 %
90 °C		100±11	12.1 %
110 °C		0	0.0 %

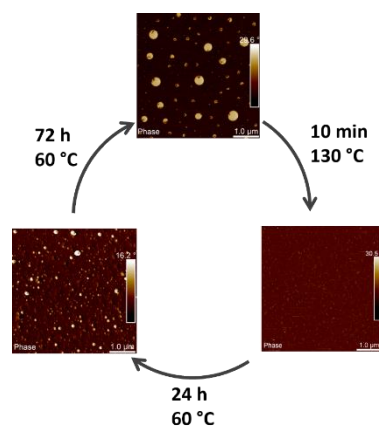


Figure S27. Cyclability of Phase separation. Heat treatment at 130 °C completely erases phase separation. Heat treatment at 60 °C for 24 h partially recovers the morphology. A fully developed morphology was found for 72 h of heat treatment at 60 °C

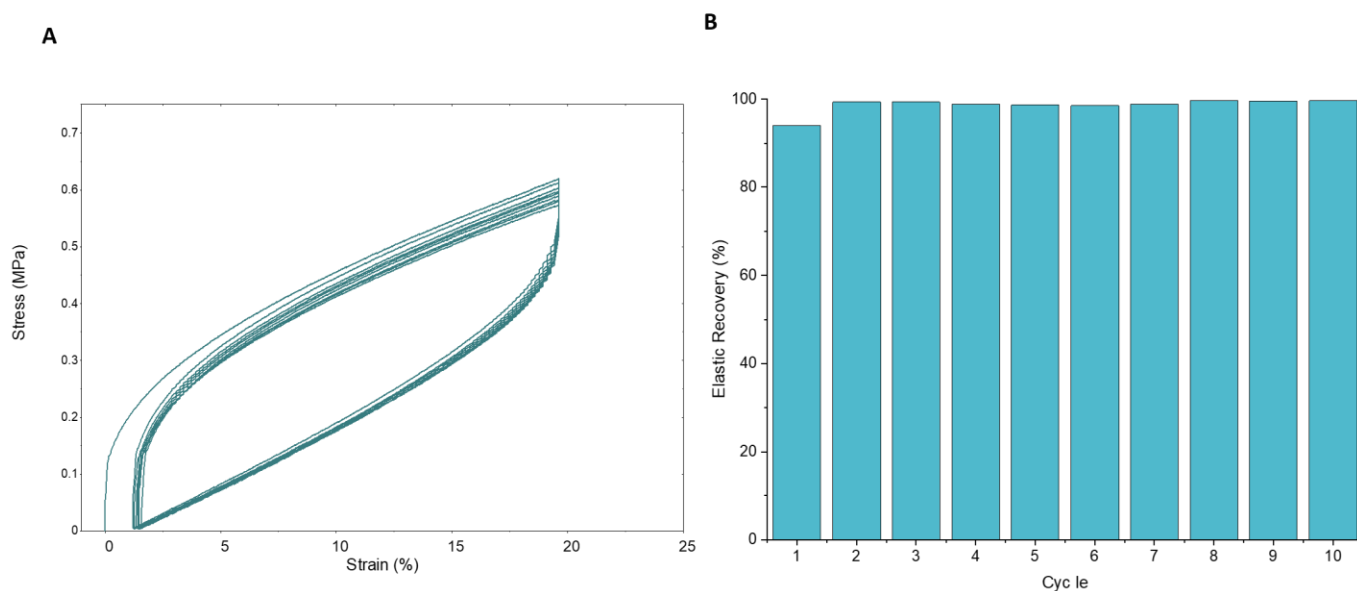


Figure S28. Hysteresis of T_S4 treated at 110 °C for 24 h over 10 cycles at 20% strain and elastic recovery.

Table S3 Mechanical properties of radical and tandem materials with a variety of crosslinkers

<i>Material</i>	<i>Crosslinker</i>	<i>T_{Anneal}</i>	<i>E (MPa)</i>	<i>ε break (%)</i>	<i>σ break (MPa)</i>
Tandem	S3	25 °C	22.9 ± 2.7	92 ± 6	12.4 ± 3.3
	S3	60 °C	6±0.3	97±10	5±1
	S4	25 °C	1640 ± 75	44 ± 3	21 ± 1
	S4	40 °C	1840±130	3.8±0.2	44±2
	S4	60 °C	3000±180	2.5±0.3	55±6
	S4	75 °C	1010±140	12.5±2.1	15.5±1.5
	S4	90 °C	11.7±1.6	88±2	7.7±1.1
	S4	110 °C	2.0±0.3	108±8	2±0.2
	S6	25 °C	1980 ± 224	4.1 ± 0.4	60 ± 5
	S6	60 °C	3300±220	2.2±0.4	70±4
Radical	S3	60 °C	8±1.5	75±9	3.9±0.2
	S4	60 °C	750±80	26±2	13±3
	S6	60 °C	1720±70	4±1	27±5

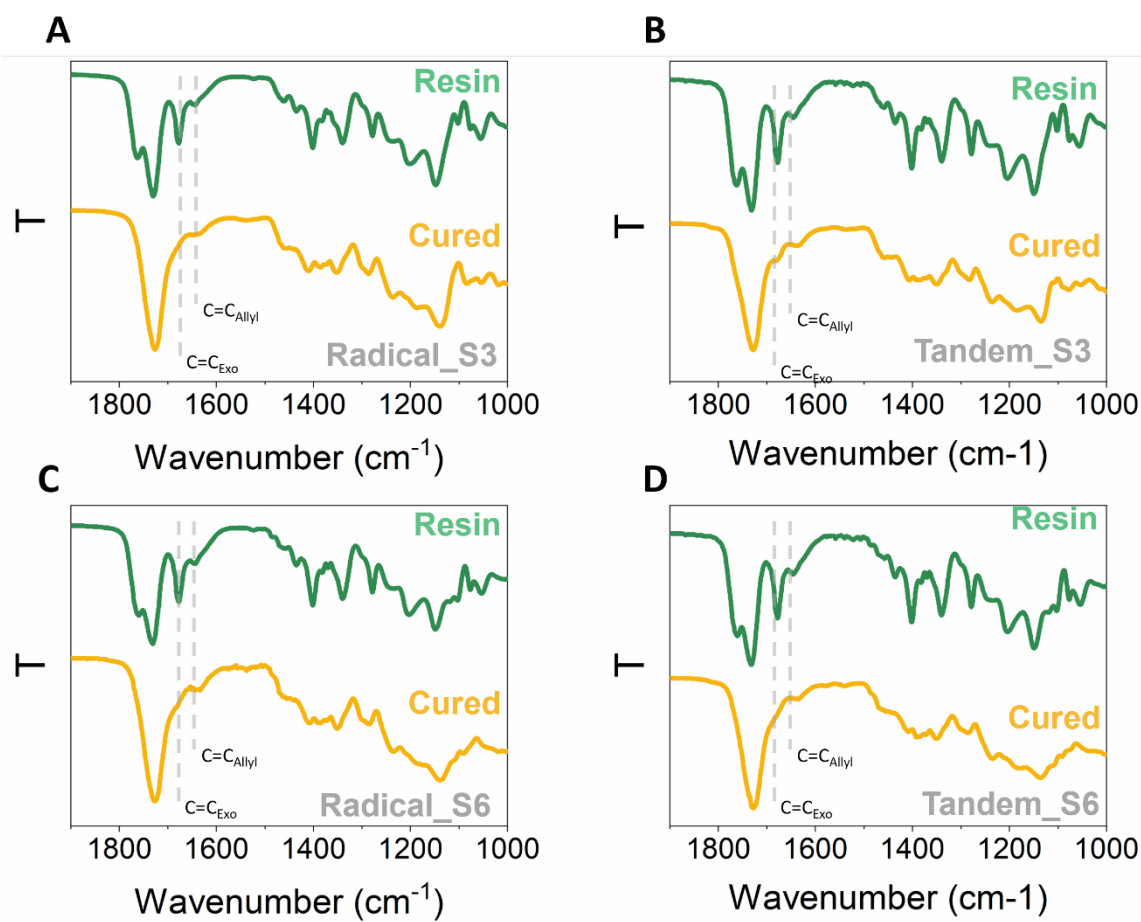
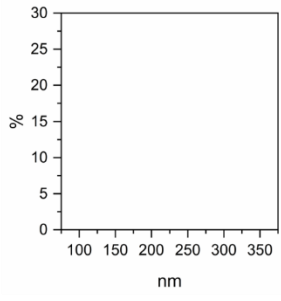
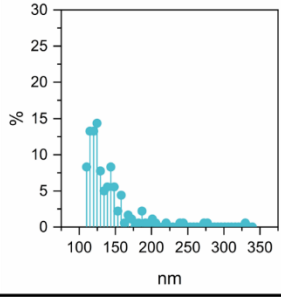
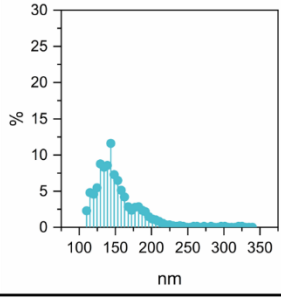
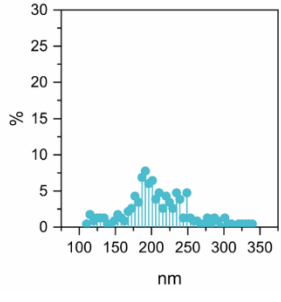


Figure S29. (a) IR pre and post curing of Radical_S3 (b) IR pre and post curing of Tandem_S3 (c) IR pre and post curing of Radical_S6 (d) IR pre and post curing of Tandem_S6

Table S4 AFM Characterization of Tandem Material prepared with Tri- and Hexathiol crosslinkers together with morphological details

Thiol	Heat Treatment (24 h)	Particle Distribution	Mean Domain diameter (nm)	Area Hard Domain (%)
Trithiol	25		-	-
	60		47±9	2%
Hexathiol	25		84±11	6 %
	60		267±54	15 %

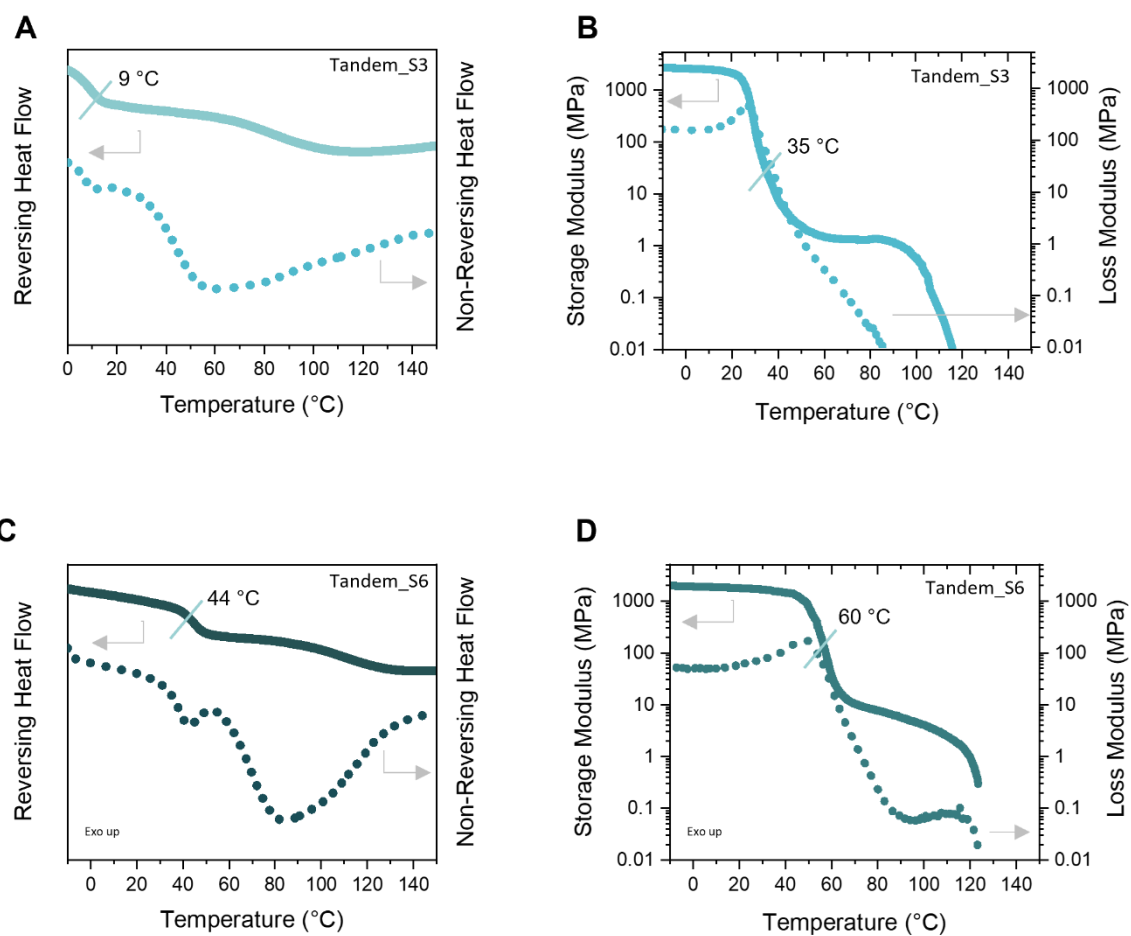


Figure S30. (a) mDSC trace of Tandem_S3 (b) DMTA trace Tandem_S3 (c) mDSC trace of Tandem_S3 T_S6 (d) DMTA trace Tandem_S6

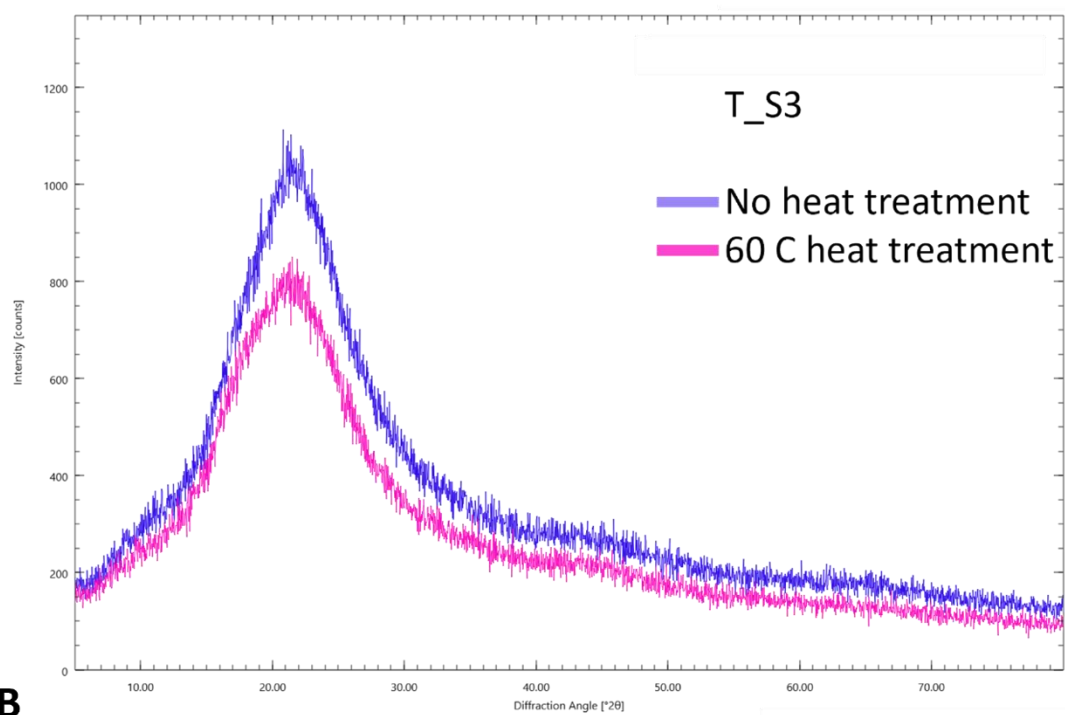
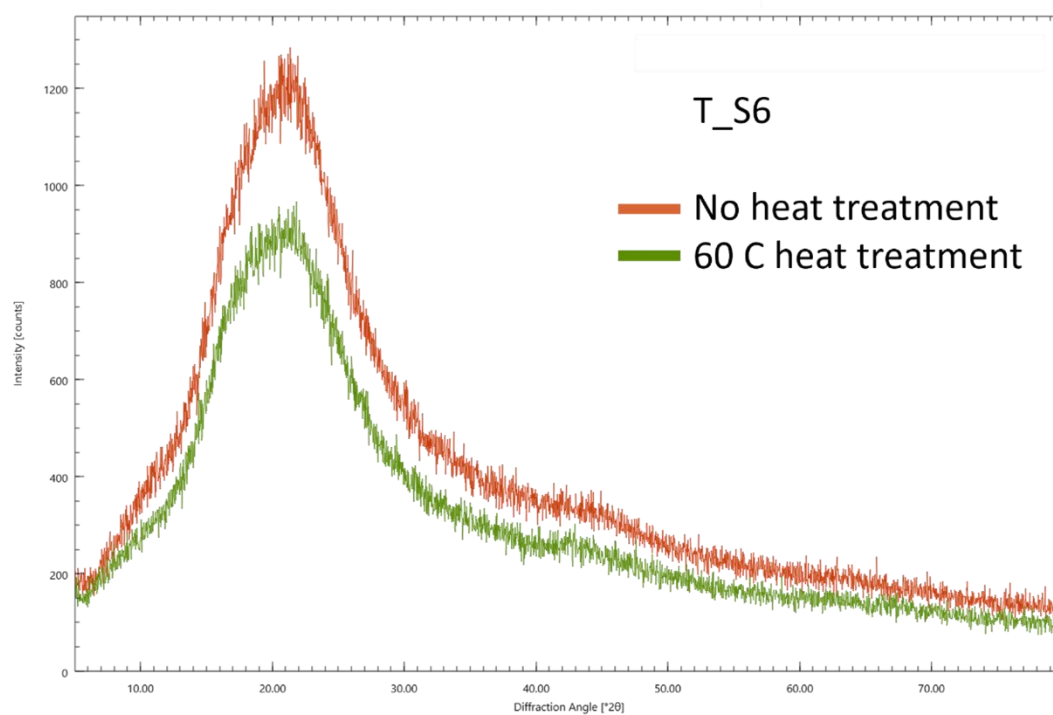
A**B**

Figure S31. XRD diffractograms of T_S3 (top) and T_S6 (Bottom)

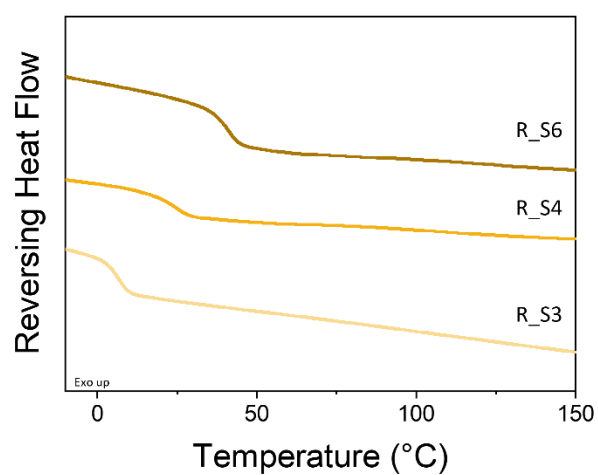


Figure S32. mDSC of R_S3, R_S4 and R_S6

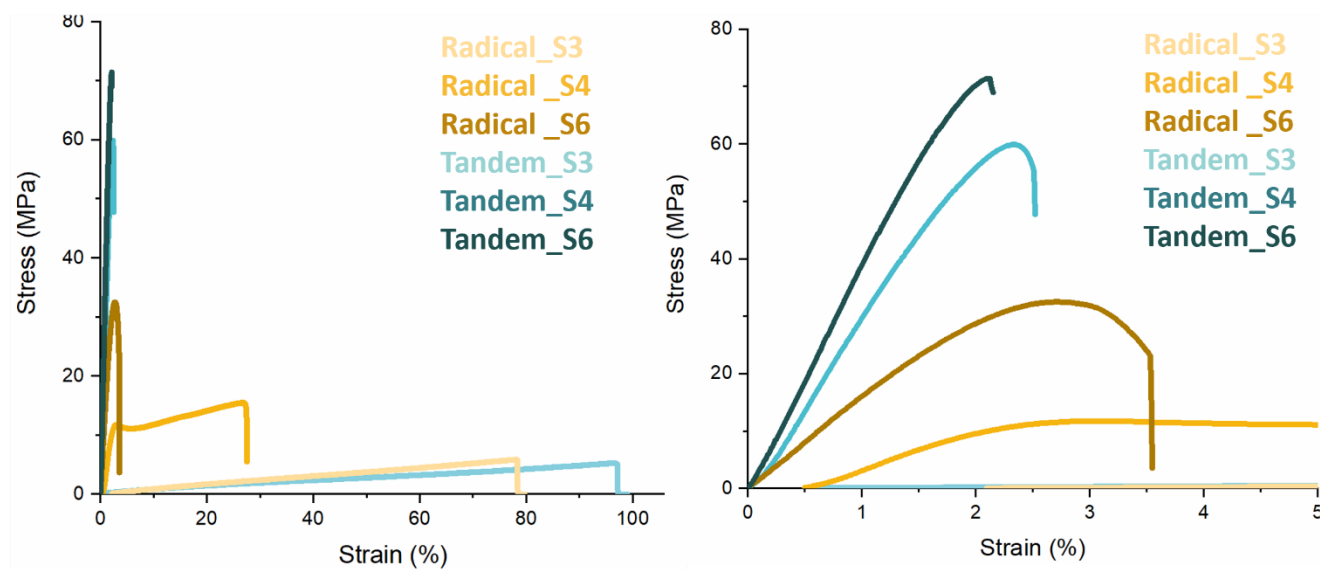
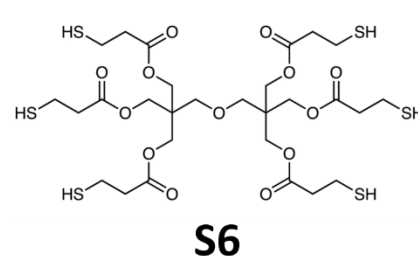
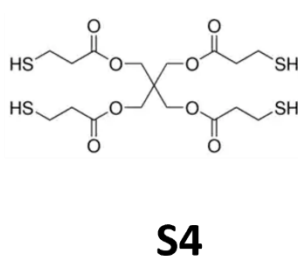
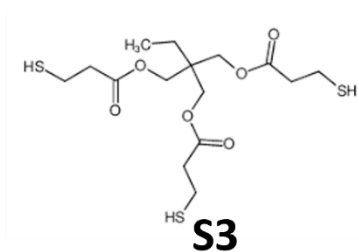


Figure S33. Top, Structures of used crosslinkers; Bottom, (left) Mechanical properties of tandem and radical materials; (right) Zoom of left graph. All materials were annealed at 60 °C for 24 h and then stored at 25 °C for 24 h before testing.

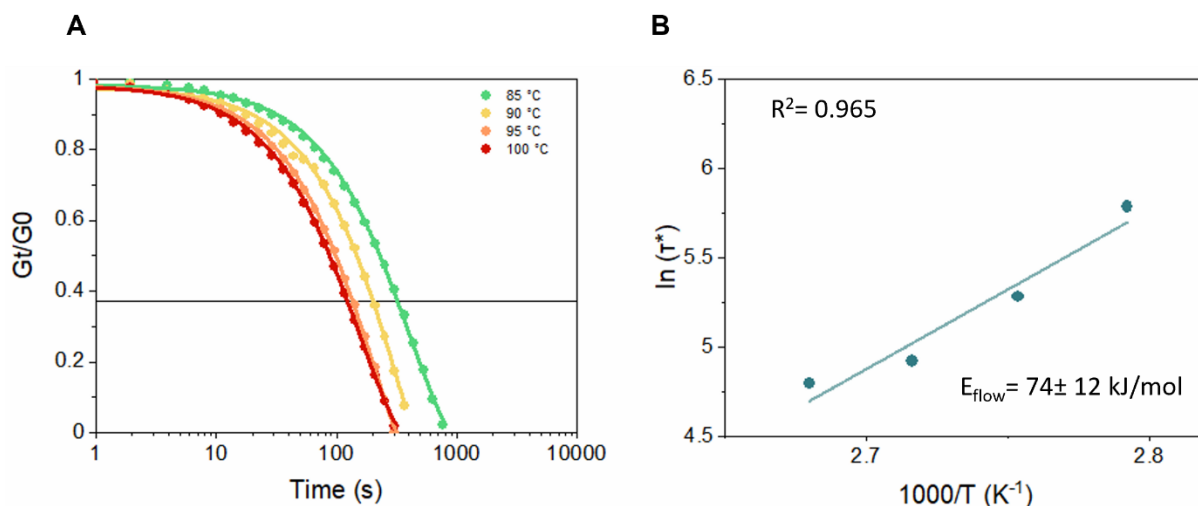


Figure S34. (a) Stress relaxation curves and first order Maxwellian fitting of Tandem_S4 after heat treatment at 110 °C (b) Arrhenius plot of Tandem_S4 heat treated at 110 °C for 24 h

Table S5 Stress relaxation data for T_S4 for different heat treatments and relative R^2 (first order Maxwellian fitting)

Sample	T (°C)	τ (s)	R^2
T_S4 60 °C, 24 h	70	1161	0.999
T_S4 60 °C, 24 h	75	872	0.998
T_S4 60 °C, 24 h	80	670	0.998
T_S4 60 °C, 24 h	85	418	0.997
T_S4 60 °C, 24 h	90	320	0.997
T_S4 60 °C, 24 h	100	165	0.999
T_S4 60 °C, 24 h	105	104	0.998
T_S4 110 °C, 24 h	85	324	0.999
T_S4 110 °C, 24 h	90	196	0.998
T_S4 110 °C, 24 h	95	136	0.999
T_S4 110 °C, 24 h	100	121	0.999

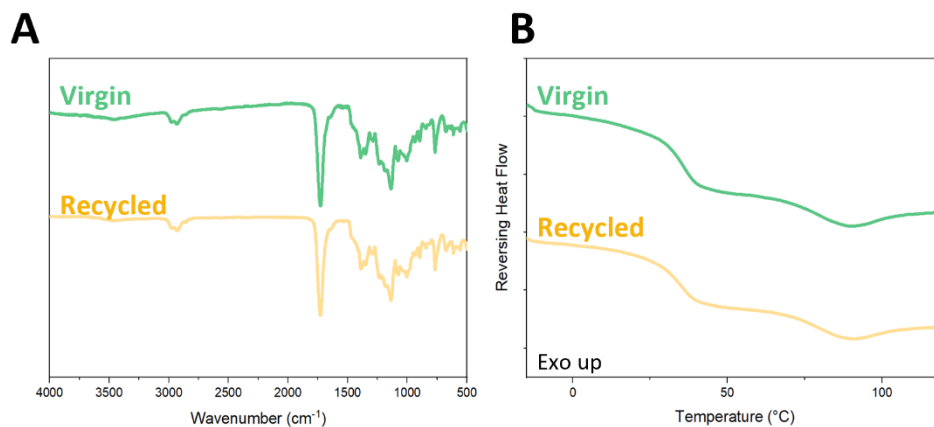


Figure S35. (a) IR Spectra of virgin and recycled materials (Tandem_S4) (b) and mDSC traces of virgin and recycled materials (Tandem_S4).

S4 3D printing

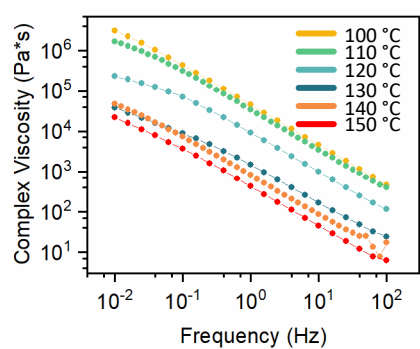


Figure S36. Frequency Sweep Rheometry (SAOS) of T_S4 at temperatures ranging from 100 to 150 °C

T_S6

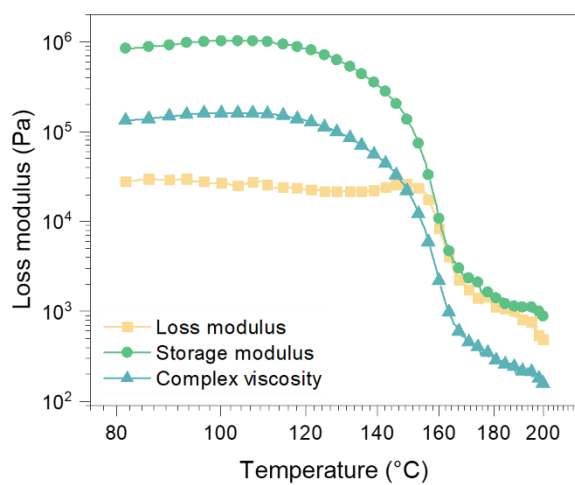


Figure S37. Temperature Sweep of Tandem_S6

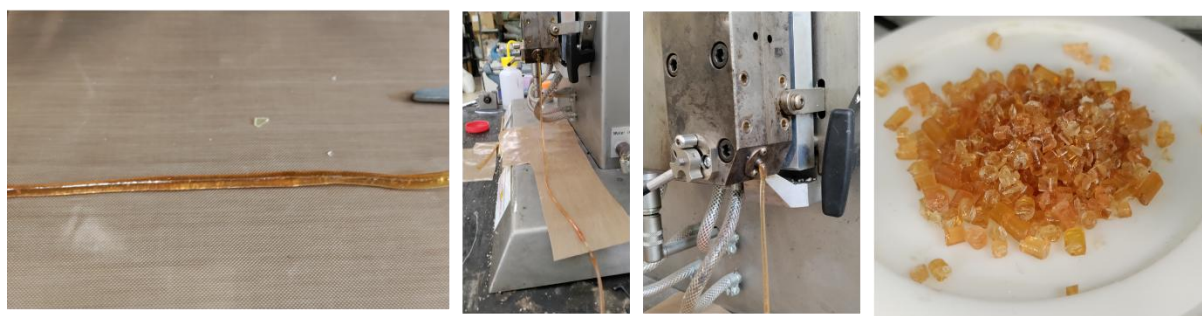


Figure S38. Filament produced from the twin screw extruder and pellets (T_S6).

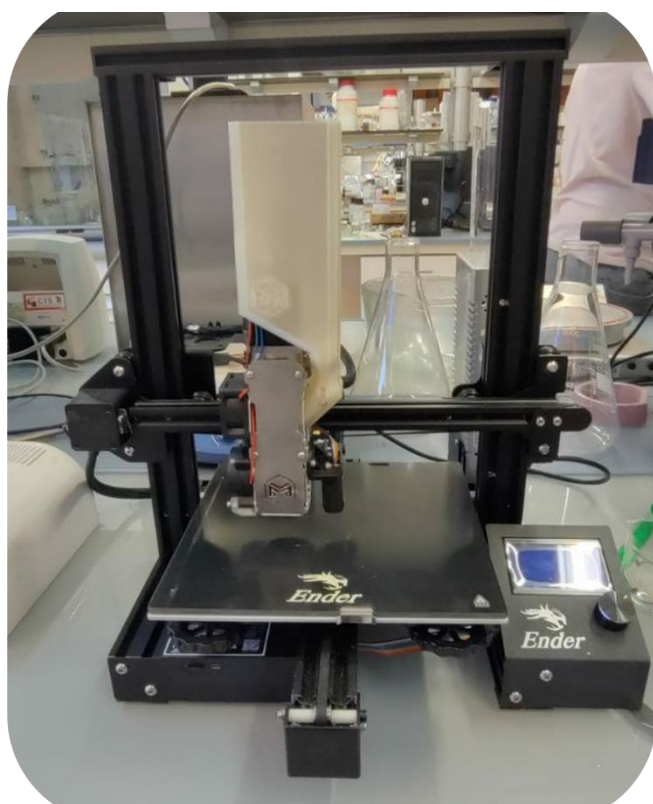


Figure S39. Ender 3 NEO 3D printer with a v4 Universal Pellet Extruder mount

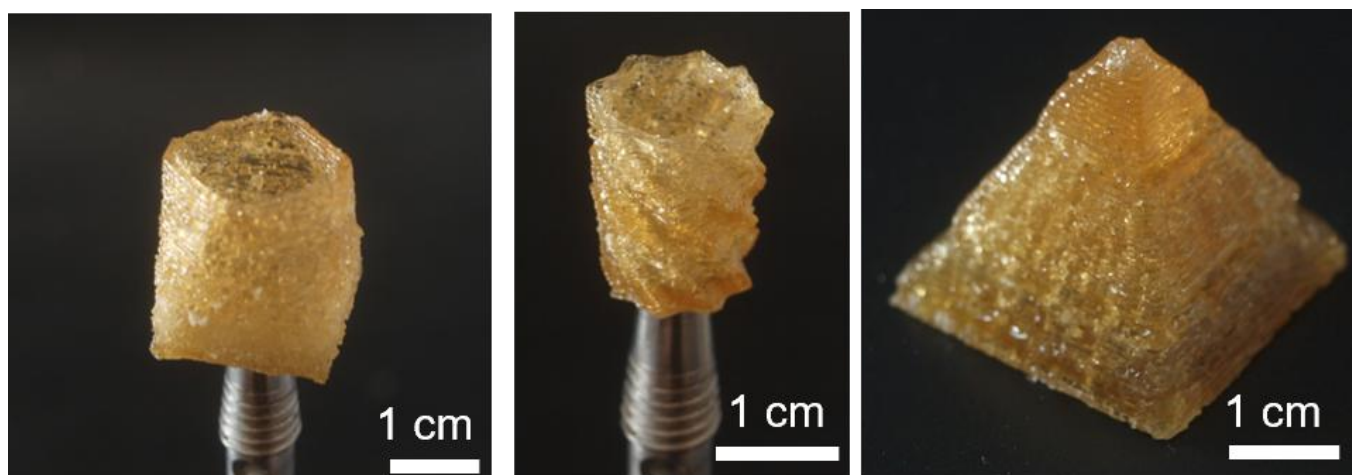


Figure S40. 3D printed structures using T_S6

References

1. Jiang, H., Zhao, J. & Wang, A. An efficient and eco-friendly process for the conversion of carbon dioxide into oxazolones and oxazolidinones under supercritical conditions. *Synthesis (Stuttg)*. **5**, 763–769 (2008).
2. Dicks, A. P. & Hent, A. Atom Economy and Reaction Mass Efficiency. 17–44 (2015) doi:10.1007/978-3-319-10500-0_2.
3. Gregory, G. L. *et al.* Triblock polyester thermoplastic elastomers with semi-aromatic polymer end blocks by ring-opening copolymerization. *Chem. Sci.* **11**, 6567–6581 (2020).
4. jcpassieux/pyxel: pyxel v1.0. doi:10.5281/ZENODO.4654018.
5. Passieux, J. C. & Bouclier, R. Classic and inverse compositional Gauss-Newton in global DIC. *Int. J. Numer. Methods Eng.* **119**, 453–468 (2019).